Conversion of Toxic Hexavalent Chromium to Trivalent Chromium by Rhamnolipid Stabilized Zero Valent Iron Nanoparticles

Fatima Nasser

Masters of Research

Human and Environmental Impacts of
Nanoscience and Nanotechnology

2012

University of Birmingham

Abstract

Zero valent iron nanoparticles (nZVI) are being used in environmental remediation of contaminants due to their reducing properties. Toxic chemicals such as hexavalent chromium (Cr(VI)) are released into environmental waters from industrial effluent and are capable of triggering life threatening diseases in humans. Solution phase Cr(VI) has can be converted to less harmful trivalent chromium (Cr(III)) using nZVI, which decreases the oxidation state. Cr(III) binds to iron and can be removed, thereby decreasing the concentration of solution phase Cr(VI). The nZVI have a high specific surface area though aggregate in solution which decreases specific surface area. In this study rhamnolipid surfactant capped nZVI of 50 nm were synthesized and were compared to nZVI without any incorporated surfactant using various characterization methods. At 10mg/L rhamnolipid incorporated nZVI and maintained a core size of 50 nm whilst raw nZVI z-average diameter increases from 341 nm to 1993 nm forming micron sized nZVI aggregates. It was determined that 1 gram of micro sized nZVI was able to convert 3 mg of Cr(VI) whilst 1 gram of nZVI was able to convert 36 mg in the same time period indicating that rhamnolipid was able to disperse particles and increase efficiency of the reaction.

Acknowledgments

I would sincerely like to thank my supervisor Professor Jamie Lead for his extensive guidance, help and enthusiasm in my project throughout the degree.

I would also like to thank Dr. Ruth Merrifield for her support, excellent advice on a variety of subjects and help with using TEM. Thank you to Dr. Mohammad Baalousha for his training on AFM, direction and encouragement. To Dr. Born Stolpe for his helpful advice. Thank you to the whole research group especially; Mila Tejamaya, Laura Ellis, William How and Marie-France Belinga for their positive attitudes, excellent ideas towards the project and supportive advice. Many thanks to Dr. Michala Pettitt for her time and help with the project.

I would like to extend many thanks to Adam Davis and Dr. Christine Elgy who have taken the time to help with laboratory equipment, share their advice and give their support in every aspect.

Table of Contents

List of Figures

List of Tables

1. Introduction

1.1 The field of Nanotechnology

The field of nanotechnology is rapidly expanding and is reaching domains such as medicine (Boisseau and Loubaton, 2011), electronics (Subramanian, 2012) and environmental remediation (Crane et al, 2011). Nanomaterials come in a variety of forms and carry out an array of functions forming a multi-billion dollar industry (Byrappa et al, 2008). Some of the leading nanomaterials are materials such as Carbon Nanotubes (CNT), which are cylinders of carbon that are utilised in a range of applications such as being used as shuttles to transport medication in the field of drug delivery (Karchemski et al, 2012). Silver nanoparticles have been used as antibacterial agents due to their disinfecting qualities (Quang et al, 2011). Titanium dioxide nanoparticles have been embedded into a range of products such as sunscreen and cosmetics (Chen et al, 2011). Many of these materials have been used throughout history in a non-nano form, as the substance itself is what carries out the desired effect, though only in the recent years has the expansion of the nano phenomenon taken these materials and made them into nano size in order to increase their efficiency by having an increased surface area for the particle to be able to interact with its surroundings.

1.2 Describing a Nanoparticle

Considering the vast amount of nano-related products available on the market, it is crucial to have an exact definition for the word nanoparticle. Different versions of the word have been derived, though the most common theme is that a nanomaterial is a material where one dimension lies in the range of 1-100 nm and has a distinctive property or chemical content. The European Commission has derived a commonly used definition of a nanomaterial: “A natural, incidental or

manufactured material containing particles, in an unbound state or as an aggregate or as an agglomerate and where, for 50% or more of the particles in the number size distribution, one or more external dimensions is in the size range 1nm-100nm". Nanomaterials are also known to be uniquely different compared to their bulk forms due to their size, shape and geometric structure (Kreyling et al, 2010) which provide novel characteristics arising at the nanoscale level such as electronic, optical and magnetic properties. The non-bulk features of nanoparticles such as their unique surface structure as well as reactivity are what give rise to enhanced dissolution, redox reactions or the creation of reactive oxygen species (Auffan et al, 2009). Nanomaterials are the highlight of upcoming science and technology for a number of reasons. Firstly, their small size is in the same range of many biochemical, electrical and physical entities such as DNA within cells (Liu et al, 2011) which make it easier for them to interact with cellular components compared to larger materials. The second quality that makes nanomaterials so novel in their uses is having a high specific surface area (Tominaka et al, 2010). Larger sized particles that are not on a nano scale have a small surface area which limits their ability to maximize their interaction with their surroundings. By decreasing the size of the particle, contingently the specific surface area drastically increases, thereby increasing the amount of atoms available to react with the surroundings which increases rates and efficiency of reactions. This is especially important with respect to semi-conductors in which spatial constraint electronic properties are important as they have many weak as well as uncoordinated bonds as well as high surface energy.

1.3 Classification of Nanomaterials

Nanoparticles can either form naturally by the environment; released as a by-product of other reactions; or can be industrially manufactured to possess specific properties which can then be

exploited for further use. Naturally formed nanoparticles are created by the environment where an example can be seen in the smallest fraction of a colloid, which is a combination of various chemical and biological phases in the nano range (Baalousha and Lead, 2007). Nanoparticles can also be created in side reactions such as during the process of combustion (Guzman et al, 2006) and can be detected in large quantities in the exhaust released by motor vehicles (Du and Yu, 2006). The third way that nanoparticles can be created is by purposely manufacturing them and they can be produced with a wide variety of chemical compositions such as silver, gold and zero valent iron, they can come in a broad range of shapes and can take on different surface groups.

There are various synthesis techniques to create different nanoparticles and parameters can be changed in order to control the size and shape of the final product. Synthesis methods can be differentiated into two major approaches, the first is the top down approach in which large structures are etched or milled to create smaller sized nanoparticles and laser ablation is a technique in the top down approach (Drmosh et al, 2010). The pulsed laser ablation method is a broadly used means to synthesize nanoparticles due to its simplicity and low cost maintenance. Parameters such as wavelength, laser pulse and pH can also be controlled to ensure a specific size of nanoparticle is created that possesses specific properties (Drmosh et al, 2010). This process uses a laser which is irradiated whereby the beam is then split and refracted through a lens before targeting the solution of metal to create the desired nanoparticle in a simple and clean fashion (Gondal et al, 2012).

The second major synthesis approach is the bottom up approach where molecules are built up on top of each other to create a larger product (Drmosh et al, 2010). One of the major benefit of the

bottom up approach compared to the top down method is that that there is more control of nanoparticle properties where in the top down approach there is limited control of the size, shape, polydispersity as well as the density of the nanoparticles. Being able to control the parameters of nanoparticles is important as the structure and size can have a drastic impact on the characteristics of the nanoparticle (Thakkar et al, 2010).

1.4 Nanoparticle Incorporation in Science and Technology

Considering the vast advantages that nanoparticles bring as opposed to their bulk counterparts such as increased reactivity, nanomaterials have been the basis of a wide variety of technology and are incorporated in many different products available on the market and sales in nanotechnology based products have increased and can be seen in figure 1.1. With respect to science and medicine, there is a drastic acceleration of publications and patents on products (Compano and Hullmann, 2002).

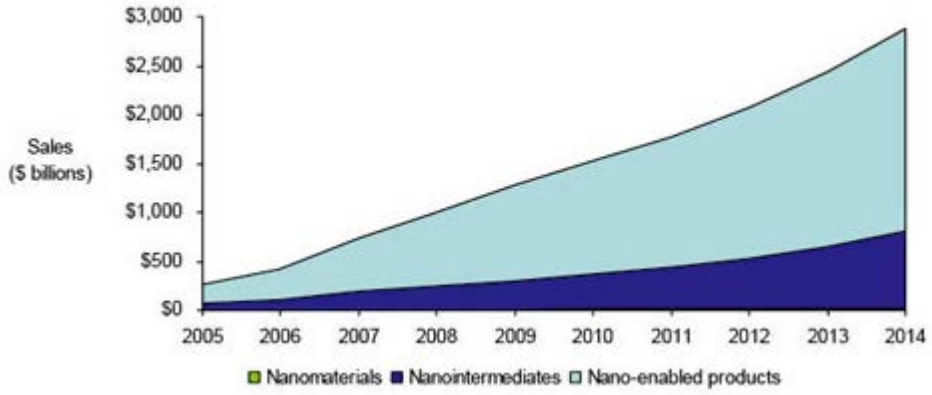

Figure 1.1. Sale of nanomaterial incorporated products being sold in the market according to Lux Research Nanomaterials Intelligence (http://www.luxresearchinc.com)

1.5 Zero Valent Iron Nanoparticles in Environmental Remediation

With the considerable amount of benefits that nanoparticles have taken part in the recent world of science and technology, it was inevitable that nanoparticles would eventually be manipulated to benefit the environment. Zero valent iron nanoparticles (nZVI) are within the very first nanoparticles that have taken part in the environmental sector and are being used to remediate environmental contaminants, due to their convenient and powerful ability to lower the oxidation state of chemicals (Li et al, 2006). This unique nanoparticle consists of two distinct parts, the inner core that consists of the metallic zero valent iron and the shell that consists of iron oxide as can be seen in figure 1.2. The nZVI has the ability to be involved in Reduction-Oxidation (Redox) reactions and is able to reduce certain chemicals such as hexavalent chromium (Cr(VI)) and organic pollutants to a less harmful form which is the precise case with Cr(VI) which is converted to trivalent chromium (Cr(III)). The rate of reaction can be accelerated with bimetallic nZVI due to a small amount of catalytic metal such as platinum or copper being imbedded into the nZVI (Chen et al, 2011).

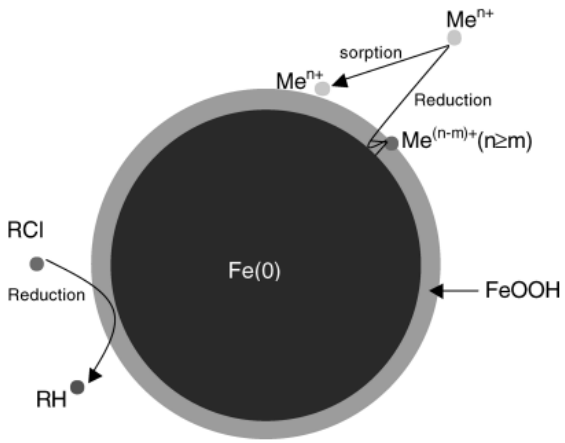

Figure 1.2. The structure of a zero valent iron nanoparticle and the various reduction reactions it may undergo with environmental pollutants (Li et al, 2006).

The core of nZVI consists of zero valent iron which is the site of electron donation in reactions. The outer shell is comprised of iron oxides and iron hydroxides that were created from the oxidation of zero valent iron. The oxidized shell provides a site for other reactions and complexes to form (Li et al, 2006). Natural organic matter (NOM) has the ability to adsorb onto an iron oxide surface by anion exchange or surface complex formation. The exchange of ligands between surface hydroxide groups and H_2O from iron oxide and the dissolved NOM gives rise to sorption on the shell (Zu et al, 1994).

1.6 Reducing the Aggregation of nZVI using Surfactants

A surfactant is an agent that is able to change the interface of a surface by changing the properties of the liquid (Llenado, 1983) The surfactant adsorbs to the surface and acts as a link between the two surfaces so that they are more compatible and thereby decreases the energy needed to assemble a new surface. Surfactants that will be used in environmental remediation should be non-toxic and eco-compatible. Surfactants can be applied to stabilize metals such as iron that are likely to aggregate and can help to disperse particles in aqueous solution in two ways. Firstly through hydrophobic and hydrophilic interactions which can give a stabilizing result. Another way that surfactants can disperse particles is through electrostatic repulsion where the charges on the surfactant repel each other thereby dispersing particles. There are many available types of surfactants and they can be divided into three categories; anionic which are negatively charged, un-ionic which possesses no charge; cationic which has a positive charge and semi-polar which has a charge placed on it (Llendado, 1983). A widely used surfactant is fulvic acid which belongs to an overarching umbrella of humic substances (HS) which are known to have ampiphillic properties and form colloids in an aqueous environment making it have the properties of a

surfactant (Tombacz and Rice, 1999). Due to their ability to be both hydrophilic and hydrophobic, HS has the capability to affect many parameters of the environment including the pH of soil, various nutrient cycles, the ability for solutes to bind to each other as well as overall human and environmental health (Thieme and Niemeyer, 1998). Due to HS ability to interact with the environment it is crucial to understand the conditions that HS is being used in as not to disrupt environmental niches.

1.7 Use of Biocompatible rhamnolipid Surfactant

The bacteria P. *aeruginosa* which is found in natural soils and water systems, has the capability of synthesizing a special glycolipid known as rhamnolipid that possess qualities of a surfactant. Rhamnolipids are composed of fatty acids linked to either a mono or di-rhamnose sugar by a glycosidic bond typical of joining sugar molecules (Soberon-Chavez et al, 2005) and can be seen in figure 1.3. Rhamnolipids are environmentally friendly; do not have any adverse effects on humans and have recently begun to replace more harmful based products in household goods such as cleaning and agricultural products due to their environmentally sound nature and thereby are termed biosurfactants. Another property rhamnolipids possess is carboxylic acid groups within their fatty acid tails which in an aqueous solution, acquire a negative charge which increases their efficiency as a surfactant by repelling other negatively charged groups through electrostatic interactions. Considering that rhamnolipids are made from a natural source, they are considered ideal surfactants in environmental remediation as there is no addition of extra chemicals into eco systems.

a.

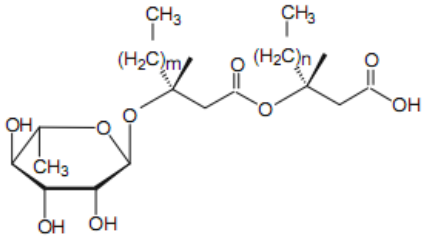

b.

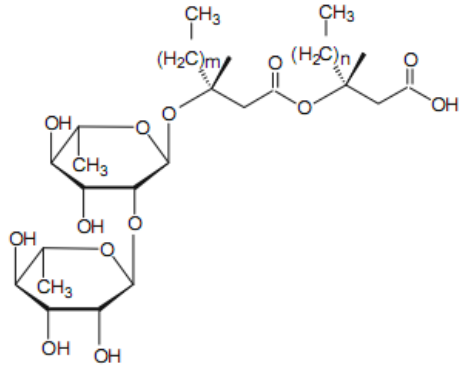

Figure 1.3. The physical structure and chemical composition of a) mono-rhamnolipid and b) di-rhamnolipids synthesized by *Pseudomonas aeruginosa* (Soberon-Chavez et al, 2005).

1.8 Hexavalent Chromium as an Environmental Pollutant

One of the key environmental contaminants is chromium due to high toxicity and high exposure from stainless steel production and plating (Permenter et al, 2011). The Canadian Council of the Ministers of the Environment (CCME) published that the limits in surface waters are 8.9µg/L for Cr(III) and 1.0µg/L for Cr(VI) while Europe environment quality standards require even lower concentrations of 3.4µg/L of total dissolved chromium (Burbridge et al, 2012). Chromium exists in three distinct forms; elemental chromium, trivalent chromium (Cr(III)) and hexavalent chromium(Cr(V)). Hexavalent chromium is a known genotoxic carcinogen that has detrimental effects on the human body. Cr(VI) has been known to be found in groundwater near areas that have industrial manufacturers of metals, leather tanneries, metal corrosion and the synthesis of

dyes and textiles. Cr(VI) is incredibly toxic, soluble and the damage imposed on humans is detrimental while Cr(III) can form a precipitate and is not as toxic (Izbicki et al, 2008).

Chromate, which has an oxidation state of six, has a very similar structure to that of sulphate and enters cells in the body using sulphate protein channels (Patra et al, 1010). Once inside the cell, Cr(VI) is reduced to a more stable pentavalent chromium which simultaneously oxidises oxygen to form reactive oxygen species (ROS) (Shi et al, 1999) which is detrimental to the body. A series of reductions take place in the cell to lower the oxidation state of pentavalent chromium by reduction to Cr(III) which is less toxic. This simultaneously creates ROS by a series of reactions such as the Fenton reaction, which in turn create a whole array of various types of ROS (Ye et al, 1999) and results in cellular damage by affecting DNA and proteins (Kanimozhi et al, 2011). A cell is able to remove certain level of ROS, as the cell itself generates some ROS to a certain degree during oxidative phosphorylation (Prete et al, 2008). Cellular protective measures such as antioxidant enzymes include super oxide dismutase, catalase and glutathione which help to redeem normal ROS levels within the cell (Jabs, 1999). ROS affects the cell by causing lipids which encompass the cell membrane to undergo peroxidation, mitochondrial damage which inevitably leads to cellular apoptosis (Ye et al, 1999). Considering the immense damage Cr(VI) can cause to humans, it is imperative to have techniques to remove Cr(VI) from drinking water that have high efficiency and low cost.

Dose dependent toxicity of Cr(VI) is important so it is vital to link short-term lab based toxicity to more long-term at-risk species in the environment. This can be done by comparing the No Observable Effect Concentration (NOEC) to the Predicted No Effect Concentration (PNEC) as

stated by the European Commission on Public Health and Risk assessment (2003). It is important to note that Cr(VI) triggers the production of ROS but cellular toxicity occurs in a dose-dependent manner (Goulle et al, 2012). Low doses of Cr(VI) will prompt low amounts of ROS to be generated within a cell which increases proliferation of the cells but still allows for cellular survival. Higher doses allow protective mechanisms of a cell to be induced which counteracts ROS production allowing the cell to survive. As the dose increases further, compartments within the cell start to become effected which eventually can lead to apoptosis of the individual cell or necrosis if the dose of Cr(VI) is drastically high. Since cellular toxicity is dependent on the concentration dose of Cr(VI), it is crucial to know environmentally relevant concentrations of Cr(VI) within the environment to gain knowledge on exposure. Literature suggests that environmentally relevant concentrations of Cr(VI) range between 0.1-10 µg/L (Ciacci et al, 2012). Knowing hazardous concentrations allows for measures to be taken to decrease the amount of dangerous chemical that is present in the environment so that ecological factors and humans are affected as little as possible.

1.9 Historical Hexavalent Chromium Contamination Sites

Numerous cases of Cr(VI) contamination from industrial sites have been reported worldwide. In Hinkley California, drinking water was severely contaminated by Cr(VI) which was used to reduce the amount of corroding metal in water cooling towers. The discharge water was then transferred to nearby ponds which seeped into water reserves that were used for drinking water for nearby residential areas. The contamination of Cr(VI) in the water led to serious illnesses of the residents, where the diseases included breast cancer, Hodgkin's disease, kidney tumours as well as miscarriages according to San Fransisco Post report on this topic. Another case of Cr(VI)

being polluted into natural waters and causing adverse health effects resulting in death was in Oinofito, Greece. The leaking of Cr(VI) into water systems caused a total of 474 deaths (Linos et al, 2011). These historical events of Cr(VI) contamination leads to the need to develop efficient methods of removing the toxic chemical from environmental systems.

1.10 Conventional versus nZVI Removal of Hexavalent Chromium

Conventionally Cr(VI) has been reduced (lowering of oxidation state) to Cr(III) by a ferrous reducing agent which leads to Cr(III) precipitating out of solution and can therefore be separated and removed from the rest of the solution phase Cr(VI).

$$Cr(VI)_{(aq)} + 3Fe(II)_{(aq)} \rightarrow Cr(III)_{(s)} + 3Fe(III)_{(s)} \qquad \text{Equation 1.1}$$

The above reaction is the typical method of reducing Cr(VI) by Fe(II) (Whittleston, 2009). Fe(II) is incorporated within a range of materials such as Fe(II) goethite, Fe(II) containing hematite and iron sulfides, which allow for a selection of materials that can be used. Interestingly, the amount of information on the kinetics of Cr(VI) is very limited though several sources suggest that the rate can be influenced by various factors such as pH as well as any organic functional groups that are in solution (Zhang et al, 2011). Reduction of Cr(VI) by Fe(II) is governed by the following rate law equation:

$$v = kA_s[M_e] \qquad \text{Equation 1.2}$$

Where v is the rate of the reaction, k is the rate constant, [M_e] is the concentration of the chromium metal present and A is the surface area of the iron particles (Ponder et al, 2000). By decreasing the size of a particle, the surface area drastically increases and therefore will increase the reaction speed in the conversion of Cr(VI) to Cr(III).

The high specific surface area of nZVI provides high reactivity of the nanoparticle towards Cr(VI) which makes it an excellent method in environmental remediation. Reactivity, however is not the only component that needs to be involved in nZVI efficiency as it must be easily dispersed so that it can travel with ease through water based filters in areas of Cr(VI) contamination. NZVI has poor mobility and literature suggests that uncoated particles can only travel mere centimetres (Li et al, 2006) with other studies indicating maximum transport distances of only a few meters (Crane and Scott, 2012) which is not ideal for sites that require remediation. One of the reasons that nZVI can not stay in solution and has such poor mobility is due to the high rate of aggregation nZVI possesses (Raychoudhury et al, 2012).

Particles that are able to remain dispersed in solution are known to have excellent colloidal stability. For particles to maintain colloidal stability there must be an energy barrier present between the various particles. When nZVI is exposed to water, the nanoparticles gain an iron oxide shell (Li et al, 2006) in which both the zero valent iron core as well as the iron oxide shell are both electrostatic which increases the attraction between particles. Particles also aggregate under environmental conditions due to pH, ionic strength and cation valency, where regular attraction between the nanoparticles results in clusters of nanoparticles quickly aggregating leading to larger particle sizes. When the nanoparticles aggregate to form the larger sized micro

particles, the specific area of the particles drastically decreases and thereby reduces the reaction rate of the conversion of Cr(VI) to Cr(III). Though nZVI have excellent ability to reduce this environmental contaminant, the fact that the nanoparticles aggregate so quickly is a downside and inevitably can decrease the efficiency as an environmental remediation method. Polyelectolyte or polymer coatings have the ability to decrease nZVI aggregation when repulsion forces overcome magnetic and weak van der Waal forces between particles (Raychoudhury et al, 2012). Coatings can reduce aggregation and simultaneously can affect reactivity (Rusch et al, 2010).

1.11 The Involvement of nZVI in Contamination Projects

NZVI has the ability to remove both organic and inorganic contaminants (Crane et al, 2011). Organic contaminants found in water such as chlorinated solvents or chlorine based pesticides have the ability to be degraded by nZVI. The nanoparticle is able to donate electrons and the chlorinated hydrocarbon receives the electrons and is simultaneously dechlorinated (Vogel TM., et al, 1987). There are a substantial number of organic environmental contaminants that can be eliminated using nZVI some of which are chlorinated methanes, chlorinated benzenes and pesticides (Zhang W., 2003). There has also been a considerable amount of projects conducted on remediating inorganic contaminants such as nickel, arsenic and chromium with nZVI as the nanoparticle has the ability to reduce the heavy metal. Work has been done on removing perchlorate which is a highly dangerous organic contaminant due to its ability to remain stable. Only a limited amount of reductants are able to reduce perchlortate such as nZVI, which was able to reduce perchlorate into chloride with no major side effects compared to micro scale iron aggregated nZVI, which worked at a much slower pace (Cao J et al, 2005).

1.12. Transport of Zero Valent Iron Nanoparticles through the Environment

Since nZVI is becoming a method of interest in environmental remediation, it is important to understand the mobility for nZVI throughout various ecological sectors and its stability in water systems as well as the final fate when removing nZVI from the environment. Since nZVI has a high tendency to aggregate, it gives reason to suggest that the mobility of nZVI to be transported is relatively low and some studies suggest that nZVI can only move mere centimetres from their point of deployment (Li et al, 2006). Nanoparticles are affected by various parameters that are present in the environment such as pH, ionic strength, for charged stabilized colloids, as well as other material within the environment, which cause the attraction between nanoparticles and lead to destabilization of the nanoparticles. These factors need to be carefully examined in order to understand how nZVI will react in various environmental conditions. This can be seen in ground water usually has a high level of dissolved ions which inevitably reduces the repulsion between nZVI particles and aids particle agglomeration (Li et al, 2006). Nanoparticles can also interact with repulsive forces which lead to better dispersion and ultimately better stabilization of the nanoparticles in solution. Understanding how the transport of nZVI is affected by different factors in the environment can help to understand the final fate of nZVI after exposure to Cr(VI) in water systems so that there is no additional contamination of the environment by adding extra chemicals especially nanoparticles whose environmental impact is still being researched.

1.13 ***Aim***

To investigate if rhamnolipid incorporated zero valent iron nanoparticles remain dispersed, stable and are able to efficiently convert solution phase hexavalent chromium to chromium bound trivalent chromium more effectively than aggregated micro size zero valent iron.

1.14 ***Objectives***

To synthesize zero valent iron nanoparticles using ferric reduction method with and without the presence of rhamnolipid surfactant and compare rates of aggregation

To completely characterize the zero valent iron nanoparticles with and without the addition of rhamnolipid surfactant

To quantitatively determine the rate of conversion of solution phase Cr(VI) into Cr(III) after exposure to rhamnolipid stabilized nZVI and compare the removal efficiency of Cr(VI) after exposure to aggregated micro scale nZVI

1.15 **Hypotheses**

$H_{Null\ 1}$ With the presence of rhamnolipid surfactant nanoparticles do not remain dispersed and rate of aggregation will not decrease

H_1 With the presence of rhamnolipid surfactant nanoparticles remain dispersed and rate of aggregation will decrease

$H_{Null\ 2}$ The presence of rhamnolipid does not allow for smaller particle size and long term stability of nanoparticles

H_2 The presence of rhamnolipid allows for smaller particle size and long term stability of nanoparticles

$H_{Null\ 3}$ The rate of conversion of solution phase Cr(VI) to Cr(III) by rhamnolipid stabilized zero valent iron nanoparticles is not as efficient as the rate of conversion solution phase Cr(VI) to Cr(III) by aggregated micro size zero valent iron nanoparticles.

H_3 The rate of conversion of solution phase Cr(VI) to Cr(III) by rhamnolipid stabilized zero valent iron naonparticles is more efficient than the rate of conversion of solution phase Cr(VI) to Cr(III) by aggregated micro size zero valent iron nanoparticles.

2. Materials and Methods

2.1 Synthesis of Zero-Valent Iron Nanoparticles

2.1.1 Pure without Surfactant

Zero valent iron nanoparticles were synthesized by the reduction of Fe(III) to zero-valent iron by sodium borohydride. This technique was adapted from Yuvakkumar et al, (2011). The zero valent iron nanoparticles were prepared in ethanol and water to prevent the iron from oxidizing and is governed by the following equation:

$$2FeCl_3 + 6NaBH_4 + 18H_20 \rightarrow 2Fe^0 + 6NaCl + 6B(OH)_3 + 21H_2$$ Equation 2.1

To produce nZVI, 0.5406g of $FeCl_3.6H_20$ was dissolved in a solution containing 24mL of absolute ethanol and 4mL of DI water. The mixture was stirred vigorously using a magnetic stirrer bar on a magnetic stir plate. A second solution was prepared by adding 0.3783g of $NaBH_4$ to 100mL (0.14M) of DI water into a beaker and stirred for 10 minutes to ensure it was fully dissolved. The borohydride solution was added drop wise into the iron chloride solution using a burette at a rate of one drop every three seconds with forceful stirring. When the first drop of borohydride is added to the iron chloride solution, small black particles can be seen even though the majority of the solution is bright orange. The rest of the sodium borohydride solution is added to accelerate and complete the reaction with the final solution being completely black as seen in figure 2.1.

Figure 2.1 Change in solution during the synthesis of nZVI. Left: Stirring of solution of nZVI after one drop of sodium borohydride solution into iron chloride solution. Right: All of the sodium borohydride solution has been added to the iron chloride solution.

After the entire contents of the borohydride solution had been added, the mixture was stirred for an extra 15 minutes.

The final solution was filtered using suction filtration over two sheets of 100 nm pore sized filter paper (Whatman). The black nZVI is captured on the filter paper while the liquid phase goes through the filter paper and is discarded. Traces of water surrounding the nZVI were washed with four portions of 25mL of absolute ethanol in order to keep the nZVI from oxidizing. The particles that were captured on the filter paper were removed, placed into a ceramic crucible and dried in the oven overnight at 323K to remove any excess water. To store the nZVI, the particles were placed in a crucible and covered with a thin layer of ethanol to inhibit the particles from oxidizing and to preserve them.

2.1.2 Rhamnolipid Surfactant Incorporation

Approximately 1 mg of rhamnolipid surfactant (Sigma Aldrich) was added to the $NaBH_4$ solution so that the surfactant would be present during the synthesis process thus coating the particles.

2.2 Characterization

2.2.1 Dynamic Light Scattering (DLS)

DLS or otherwise commonly known as Photon Correlation Spectroscopy or Quasi-electric Scattering, is a widely used technique that allows the determination of the size of particles on a micro and nano scale (Malvern Instruments LTD, 2012).

Particle movement is governed by Brownian motion which states that particles in a fluid whether it is liquid or a gas, move in a random fashion due to inter-particle collisions fuelled by thermal energy. A laser is shone into the suspension containing the nanoparticles whereby the intensity of the scattered light changes depending on the size of the particles in the sample. DLS creates and autocorrelation function from the fluctuations in the scattered light with respect to time. The function decays at an exponential rate as a function of the correlator time delay which can be used to calculate the particle diffusion coefficient (Baalousha and Lead, 2012). DLS calculates the diameter of a particle also known as the hydrodynamic diameter which focuses on a particles ability to diffuse through a medium which can be seen in figure 2.2. Consecutive scattered (speckle) patterns are compared until the features no longer correlate with the original pattern. DLS determines the hydrodynamic diameter by applying the diffusion coefficient to the Stokes-Einstein equation (Baalousha and Lead, 2012). This diffusion coefficient can be greatly affected

by numerous factors; the size of the particles; any surface modifications; the concentration of the sample; the viscosity of the media; as well as any ions that may influence the nature of the particles (Malvern Instruments LTD, 2012).

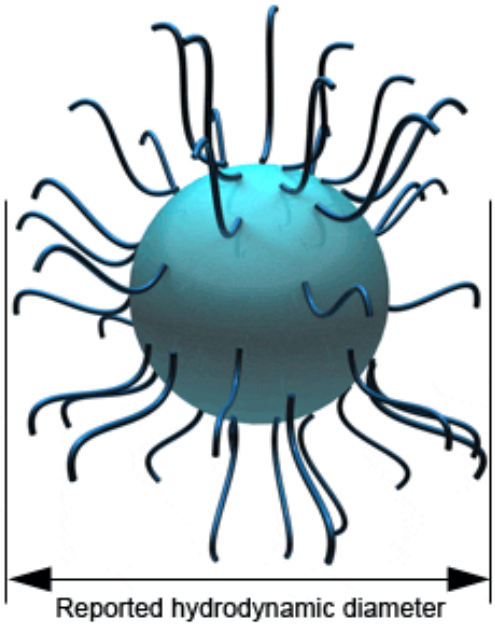

Figure 2.2 The hydrodynamic diameter of a nanoparticle which dictates how a nanoparticle is able to diffuse through a liquid (Malvern Instruments LTD, 2012)

As nanoparticles undergo thermal motion they diffuse through a medium, the scattered light goes through interference effects which can be seen in figure 2.3 which changes arbitrarily with time. As the fluctuations start to decay they can lead to information on the size of the particles where smaller particles have a much faster rate of decay (Borkovec, 2002).

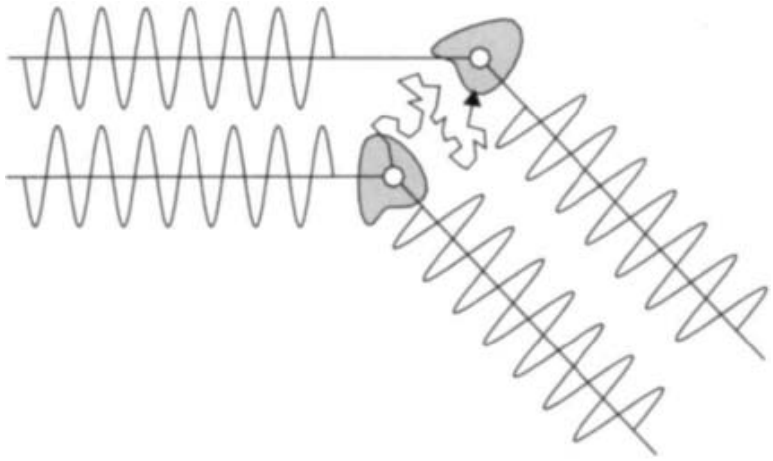

Figure 2.3 Depiction of interference patters that happen during Dynamic Light Scattering (Borkovec, 2002)

The intensity correlation of the scattered light can be easily calculated using the following function:

$$g_2(t) = \frac{\langle I(t)I(0)\rangle}{I^2} \qquad \text{Equation 2.2}$$

The above function can be related to a normalized function used for electrical fields of scattered light $g_1(t)$ which was derived from the Seigert relationship, which is as follows:

$$g_2(t) = 1 + g_1(t)^2 \qquad \text{Equation 2.3}$$

DLS does indeed measure the coefficient of diffusion of particles which is closely related to the size of the hard, spherical particle which is defined by the Stokes-Einstein equation:

$$D = \frac{k_b T}{6\pi\eta R_h} \qquad \text{Equation 2.4}$$

K_B is known as the Boltzmann constant, T is the absolute temperature, n is the viscosity of the solvent that the particles are in, R_h is the hydrodynamic radius of the particle which is the value to be determined. Since the rate of decay in the time correlation function can be measured with accuracy, the particle size can be accurately determined. DLS works most efficiently with particles that are monodispersed though moderately polydispersed samples can be analyzed using DLS as well (Borkovec, 2002), however the scattering is highly weighted towards larger particles and smaller particles may be missed.

A Standard Operating Procedure (SOP) used to measure the hydrodynamic diameter was created to set the parameters of the sample and was kept the same for all samples. The refractive index and adsorption of nZVI was set to 2.87 and 0.5 respectively. The temperature was kept at 20°C, an equilibrium time of 120 seconds for each sample as well as five readings taken per sample to ensure accuracy of the results.

The sample contained 0.05 g of nZVI suspended in 10 mL of DI water resulting in a final concentration of 5 g/L. The sample was set in an ultrasonic bath (Branson 1510) at power 9 for 30 minutes to achieve a homogeneous appearing suspension in order to make the sample as monodispersed as possible. After sonication, 720 µL of suspension was pipetted into a low volume disposable cuvette (ZEN0112) and placed within the sample holder inside the Malvern Zetasizer instrument, with the clear sides of the cuvette exposed towards the laser.

2.2.2 Zeta Potential

Zeta Potential is used to measure how stable the charge is of dispersed particles within a solution. Charged stabilized particles will have an electric double layer surrounding them as seen in figure 2.4. This double layer will have a different charged compared to the suspension media. Zeta potential determines the difference in the charge between the electric double layer and the suspension media and not the charge of the particles themselves (Malvern Instruments Ltd, 2012).

The electric double layer is formed either by the functional groups becoming ionized or charged species becoming adsorbed onto the surface of the particles (Malvern Instruments Ltd, 2012). Particles move due to Brownian motion and are kept separate from each other by the charged layer due to repulsive forces. The layer can be influenced by the concentration of ions and the pH of the suspension media. The slipping plane is the point at which the zeta potential is measured and is where the electric double layer moves past the suspension when influenced by an external known voltage. By increasing the ionic strength of the media by the addition of a salt, the electrical double layer is reduced allowing the particles to aggregate. When the pH (Metcalf and Healy, 2012) of the suspension media is altered the surface charge of the particles can take on an opposite charge. However there will be a pH in all systems at which the zeta potential is 0 and the particles aggregate, this is called the iso-electric point (Healy and Fuerstenau, 2007).

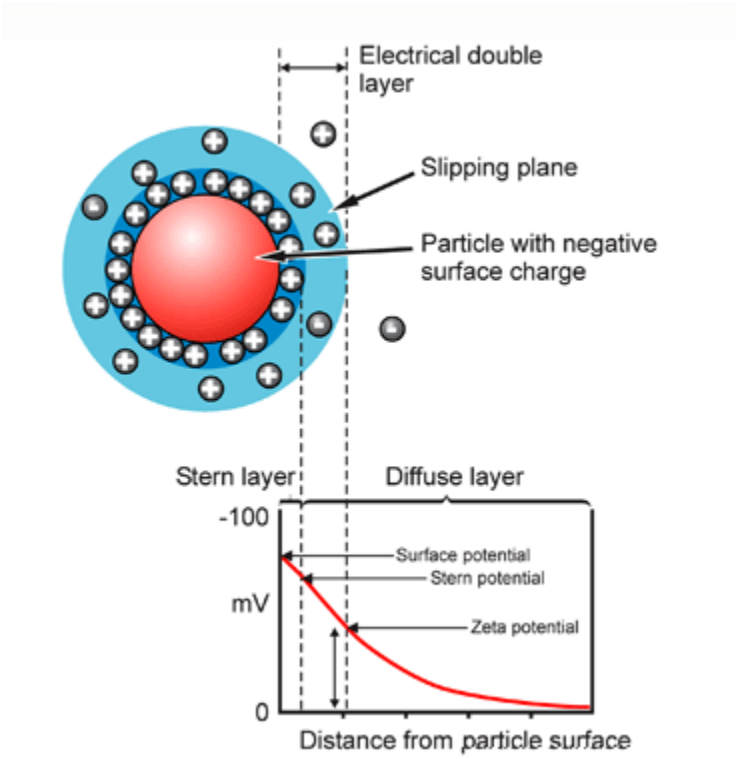

Figure 2.4 Representation of a particle with a surface charge attracting positive (Malvern Instruments Ltd, 2012)

A voltage is applied across the particle suspension so particles that have an electric double layer will be attracted toward the electrode that holds the opposite charge at a speed which is directly correlated to the absolute value of the zeta potential. This resulting speed of particles can be measured using laser Doppler velocimetry, where the moving particles cause a frequency shift in the applied laser beam and this shift is measured as the mobility of the particles which can easily be converted to zeta potential using equation 2.5. (Malvern Instruments Ltd, 2012).

$$U_E = \frac{2\varepsilon z f(ka)}{3\eta}$$ Equation 2.5

U_E is the electrophoretic mobility which is the velocity at which the particles travel at, ε is the dielectric constant, z is the zeta potential, η is the viscosity of the solvent in which the particles are suspended in and lastly f(ka) is Henry's function. In Henry's function there are two parameters used, k^{-1} is the inverse of the width of the electrical double layer formed and *a* is the radius of a particle in solution. Therefore f(ka) is 1.5 in a polar solution and 1.0 in a non-polar solution according to the Smoluchowski and Huckel approximations respectively (Malvern Instruments Ltd, 2011).

A zeta-potential specific cuvette was first rinsed with ethanol using two syringes to push and pull the fluid through and then washed with DI water five times in the same way. The sample was prepared by adding 1.0 g of nZVI to 100 mL of DI water which was then set in the ultrasonic bath on power nine for 30 minutes. The sample was then syringed into the cuvette carefully to ensure that there were no air bubbles present. The same SOP parameters were used as the DLS SOP.

To determine the Iso-electric point, the same concentration of nZVI was used and the pH was adjusted by adding HNO_3 or NaOH manually by pipette and then stirred at 100 rpm for 10 minutes to ensure proper mixing. The pH was taken by using an automatic pH meter (Thermo Orion 3 Star) and then the zeta potential was taken.

2.2.3 X-Ray Diffraction (XRD)

Structural characterization of molecules can be characterized due to techniques such as XRD. This technique is accomplished using a pump and probe method where short laser pulses induce

the reaction and a diffraction signal from an x-ray pulse alters the special relationship between atoms giving rise to a diffraction pattern (Ihee et al, 2005) and can be seen in figure 2.5. X-rays are scattered by the electron clouds of the atoms and Bragg's law links the scattering to structure (Dong and Boyd, 2011). Bragg's law is given by the following equation:

$$n\lambda = 2dsin\theta$$ Equation 2.6

The majority of solid substances can be described as crystalline. A diffraction pattern results when an x-ray is exposed to a crystalline substance. A crystalline substance can be described as a substance where the atoms are organized in a repeating pattern and the smallest repeating component is termed a unit cell. The axes of a unit cell are a, b and c and the corresponding angles are alpha, beta and gamma respectively (Scintag Inc, 1999). When x-rays scatter, the wave fields constructively or destructively interfere with each other. In crystal structures, the waves are scattered and separated by the interplanar distance (d). Constructive interference is satisfied by Braggs law where n is an integer, λ is the wavelength and θ is the angle in which the x-rays are scattered. The scattered x-rays will create intense peaks which generates a diffraction pattern (Dong and Boyd, 2011).

If an electron is moving across an electromagnetic field, the electron will start to fluctuate at the same frequency as the beam which results in destructive interference where the waves are out of sync. The atoms in a crystal are known to have a specific and repetitive pattern and therefore a few waves will have constructive interference. The waves will be in phase, x-ray beams will

leave the sample which can then be used to calculate the crystalline structure of the sample (Scintag Inc, 1999). The data base EVA was used to match crystal structures.

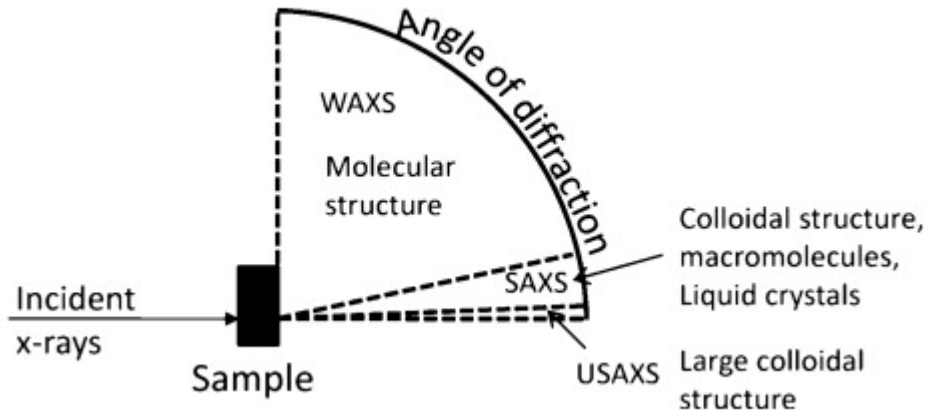

Figure 2.5 Diagram depicting x-ray beams creating scattering, resulting in diffraction (Dong and Boyd, 2011)

The International Center Diffraction Data (ICDD) is an association that keeps a record of both organic and inorganic spectra. The information provided is on spacing, cell parameters as well as a database to match the spectra of a sample to the spectra obtained by published work in order to match peaks.

A solid XRD sample holder was used and the sample was placed in the middle and pressed with a glass slide to ensure the sample was as flat as possible. The sample holder was loaded into the XRD and the XRD wizard software was opened. The parameters were set to scan from 20 to 60 Θ as the diffraction angle and the scan time was set for half an hour. The analyzing software EVA was then used to select the elements of the periodic table that had a chance of being in the

sample where iron, oxygen and hydrogen were all selected as possible candidates. An XRD of the fresh sample was taken within the first 20 minutes after the sample was synthesized.

2.2.4 UV-Visual Spectroscopy

UV-Vis is a spectroscopy technique where a beam of light bombards a sample and some light becomes absorbed into the sample while the rest is transmitted through the sample (Upstone, 2000). Percent transmittance of light can be calculated by taking into account the original intensity of light (I_o) and comparing it to the amount of light leaving the sample (I_T) with the following formula:

$$\%T = \frac{Io}{It} \times 100 \qquad \text{Equation 2.7}$$

Transmittance (T) can be converted into Absorbance (A) with the following equation:

$$A = -logT \qquad \text{Equation 2.8}$$

UV-Vis utilizes Beer Lambert's law which indicates that there is a direct and linear relationship between absorbance and concentration within the same path length (Upstone, 2000). UV spectra can then be created and nonlinearity can occur due to light within instrument that are not at analytical wavelengths. The following is Beer Lambert's law:

$$A = \varepsilon Cl \qquad \text{Equation 2.9}$$

The 6800-Jenway UV-visible spectrophotometer was used to characterize the absorption of the nanoparticles. This is a dual beam spectrophotometer where the incoming incident light is split into two beams by a silver based mirror. The light is split into a sample and reference beam. This unique design compared to other spectrophotometers reduces the necessity for mechanical beam shutting which results in an excellent baseline (Upstone, 2000).

The UV spectra were used to semi-quantitatively observe the presence of the nZVI Plasmon resonance at 268 nm. UV-vis measurements were taken using Plastibrand cuvettes, which provide a 1 cm path length and a 6800 Jenway UV-vis spectrophotometer was used. Before UV-vis data was collected on the nZVI samples, the instrument was blanked using DI water and each sample was set to replicate three times for accuracy.

2.2.5 Atomic Force Microscopy (AFM)

The atomic force microscope, invented in 1986 (Binning et al, 1986), is able to take images of molecules or even atoms. One advantage AFM provides over other microscopy techniques is that it can function on conductive, semi conductive or non-conductive samples whereas other instruments have the need for a conductive surface. AFM relies on mechanical, rather than electronic interactions between the sample and the probe (Pishkenari et al, 2006). As a probe gets closer to the sample (within a 100 nm), van der Waal's forces between the sample and the probe provide week attractive interactions and as the probe gets even closer to the sample the probe will start to repel the sample due to Lennard-Jones potential (Dill and Bromberg, 2002). The attractive or repulsive force can be measured by spring mechanics which depicts the interaction between

the tip and the sample and a contour map can be created in terms of height (Ikai A, 2008). The force is tracked by a sensor in the form of a cantilever which is a very thin spring seen in figure 2.6.

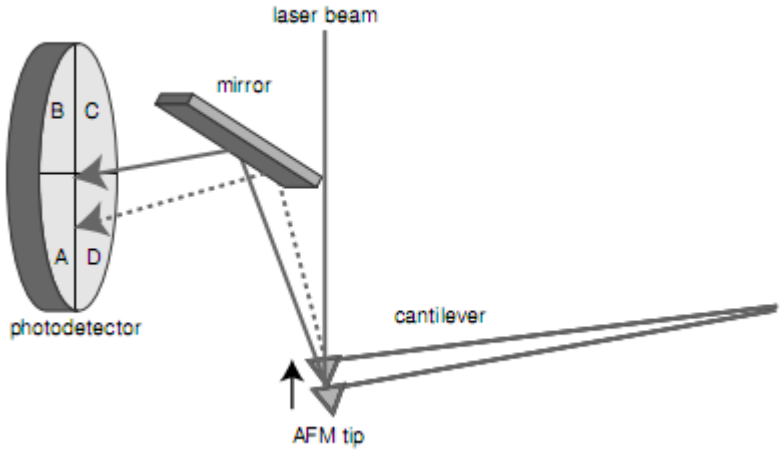

Figure 2.6 Force transduction in AFM is due to a laser beam being reflected off a cantilever and then a mirror which then reaches a photodiole detector. (A +D) – (B + C) is correlated to the deflection of the cantilever and can be used to calculate the magnitude of force (Ikai, 2008).

As the cantilever tip passes over the sample, a potential energy is generated which creates force (F_{ts}) and is governed by the following equation:

$$F_{ts} = \frac{-\partial V_{ts}}{\partial z} \qquad \text{Equation 2.10}$$

The force can include weak forces such as van der waals or stronger forces such as the Lennard-Jones potential mentioned previously as well as the Morse potential (Bhushan, 2004). The Lennard-Jones and Morse potentials depict the potential energy within chemical bonds (E_{bond})

and σ is the distance between equilibrium and k is the length of decay. The following are the two equations:

$$V_{Morse} = E_{Bond}(2e^{-k(z-\sigma)} - e^{-2k(z-\sigma)}) \quad \text{Equation 2.11}$$

$$V_{Lennard\ Jones} = E_{Bond}(2\frac{\sigma^6}{z^6} - \frac{\sigma^{12}}{z^{12}}) \quad \text{Equation 2.12}$$

A mica sheet (Agar Scientific) was taken and cut to have an area with 1cm x 1cm dimensions and cleaved into two sheets using tweezers to provide a clean and flat surface to deposit the nanoparticles on. 200µL of sample was dropped onto the shiny side of the sheet with a pipette and let to dry for a minimum of three hours. The sheet was covered to prevent any contamination from the surroundings. The sheet was then suspended in DI water for 30 seconds to remove any salt residue and then left again to dry, covered.

AFM measurements were conducted using an XE-100 AFM by Park Systems and set into the non contact mode. The cantilever (Silicon non contact, Park Systems) were used and images as well as height histograms were analyzed using XEI software. Every sample had 100 height measurements taken to ensure accuracy and a generalized area was used on the mica surface.

2.2.6 Transmission Electron Microscopy (TEM)

TEM works similarly to a light microscope though uses electrons instead of photons. The smallest observable object seen with any optical microscope is equal to the wavelength of the

electromagnetic field being used to illuminate it. The wavelength of accelerated electrons is approximately 6pm (0.006nm), which is 1000 fold smaller than the wavelength of light of approximately 600 nm (Twyman, 2005). However electron microscopes are subject to large aberrations and energy spreading so most modern microscopes have a resolution of between 0.3 – 0.2 nm. Electrons are released into the electron gun by thermionic, Schottky or by field emission (Reimer and Khol, 1997) and field emission was used to produce TEM images in this study. The wavelength of the electrons is controlled by a high voltage source which is within the TEM instrument (Zou et al, 2011) The electrons are able to interact powerfully with the atoms in the sample by elastic or inelastic scattering so it is crucial for the sample to be extremely thin (5-100 nm) depending on the density and composition of the sample (Reimer and Khol, 1997) as the electrons need to be transmitted through the sample. A beam of electrons with a narrow energy dispersion is released into a vacuum which are then concentrated by lenses. The objective lenses before and after the sample cause the beam to be homogenous across the sample. The electrons are then directed onto a screen to form a phase contrast image (Rochow and Tucker, 1994).

TEM samples were made using copper mesh grids which were coated in a holey carbon layer (Agar Scientific). The purpose of choosing these grids in particular is that the edges of the carbon layer act as a means to focus the image. TEM grids were prepared by dropping 15µL of suspended particles on the grid which had been ultrasonicated for one hour. The grid was allowed to dry for one hour and was covered to ensure there was no contamination by dust. The sample was checked periodically during this hour for any evaporation of the sample, which was replaced in order to be certain that the grid was fully exposed to the nanoparticles for a full hour. The samples were then suspended in DI water for 30 seconds to remove any excess nanoparticles and

salt formation and then re-suspended in fresh DI water for another 30 seconds and then allowed to dry covered overnight. The grids were analyzed using Technai F20 with a field emission gun having a point resolution 0.27nm and a tension o 200 Kev.

2.3 Reduction of Hexavalent Chromium

2.3.1 Flame Atomic Absorption Spectroscopy

Flame Atomic Adsorption (FAA) spectroscopy is a quantitative method for the determination of the concentration of an element in solution. FAA is prone to less error than other methods such as ICP-MS (Ferreira et al, 2001) when looking at materials in the 0.5-5 parts per million range whereas ICP-MS is accurate in the parts per trillion range depending on the element being analysed. The atoms in the sample need to be vaporized at a high temperature by a flame furnace. These atoms are then able to absorb various wavelengths and move to a higher energy level. The source of light is a hollow cathode lamp which consists of a tungsten anode as well as a cathode made out of the same material as the sample being analysed as well as an inert gas. The concentration of the sample is established from the amount of absorption of the element.

Standard curves must be created to determine the linear range for detection of the specific element. Each lamp has a certain concentration threshold to which it can detect, so standard curves need to be generated below the maximum concentration and are created using known concentrations.

Measurements were conducted with a Perkin Elmer Instruments Analyst 300 AAS with a chromium cathode lamp. The chromium lamp had a maximum threshold concentration of 5 mg/L

and therefore a standard curve was created within the linear range of the lamp with standard solutions at 1, 2, 3, 4 and 5mg/L. The standard solutions were made from a stock solution and diluted into the various concentrations.

Samples were created by diluting a 10g/L stock solution of Cr(VI) into 10 mL of 5 mg/L. Four identical samples were created and exposed to 1 gram of zero valent iron microparticle each and exposure times were 0, 1, 2, 3 and 4 hours. At the end of the exposure time the samples were put into centrifuge vials and set to centrifuge for 20 minutes at 300G. FAA was taken of the supernatant which contained the remaining Cr(VI) in aqueous phase that had not been converted into Cr(III) which becomes a solid. Parallel experiments were run with nZVI as well as a control with only Cr(VI). Each sample was set to have the concentration taken three times and averages were created to prevent inaccuracy.

3. Results

Characterization of Zero Valent Iron Nanoparticles

3.1 Pure Synthesized Nanoparticles without Surfactant

Zero valent iron nanoparticles have become the pinnacle of interest due to their numerous medical and environmental applications (Barnes et al, 2010). To understand any transformations that occur to nZVI in different environmental circumstances, it is crucial to characterize the various properties of the nanoparticles.

3.1.1 Dynamic Light Scattering

DLS was taken of the nanoparticles in order to determine the hydrodynamic diameter of nZVI at various time points. The purpose was to determine the initial size of the nanoparticle aggregate and to monitor the rate of aggregation. It was resolved that the initial size of the nanoparticle, without the use of any surfactant, was not in the nano range and the aggregate size increased over time to micron size. An outline of DLS results is indicated in Table 3.1.

Table 3.1 Hydrodynamic Diameters of nZVI aggregates over a four hour period. Diameters are Z- averages of five measurements.

Time (h)	Hydrodynamic Diameter (nm)	Polydispersity Index
0	341 ± 0.22	0.221
1	840 ± 0.34	0.322
2	1370 ± 0.25	0.384
3	1993 ± 0.43	0.395

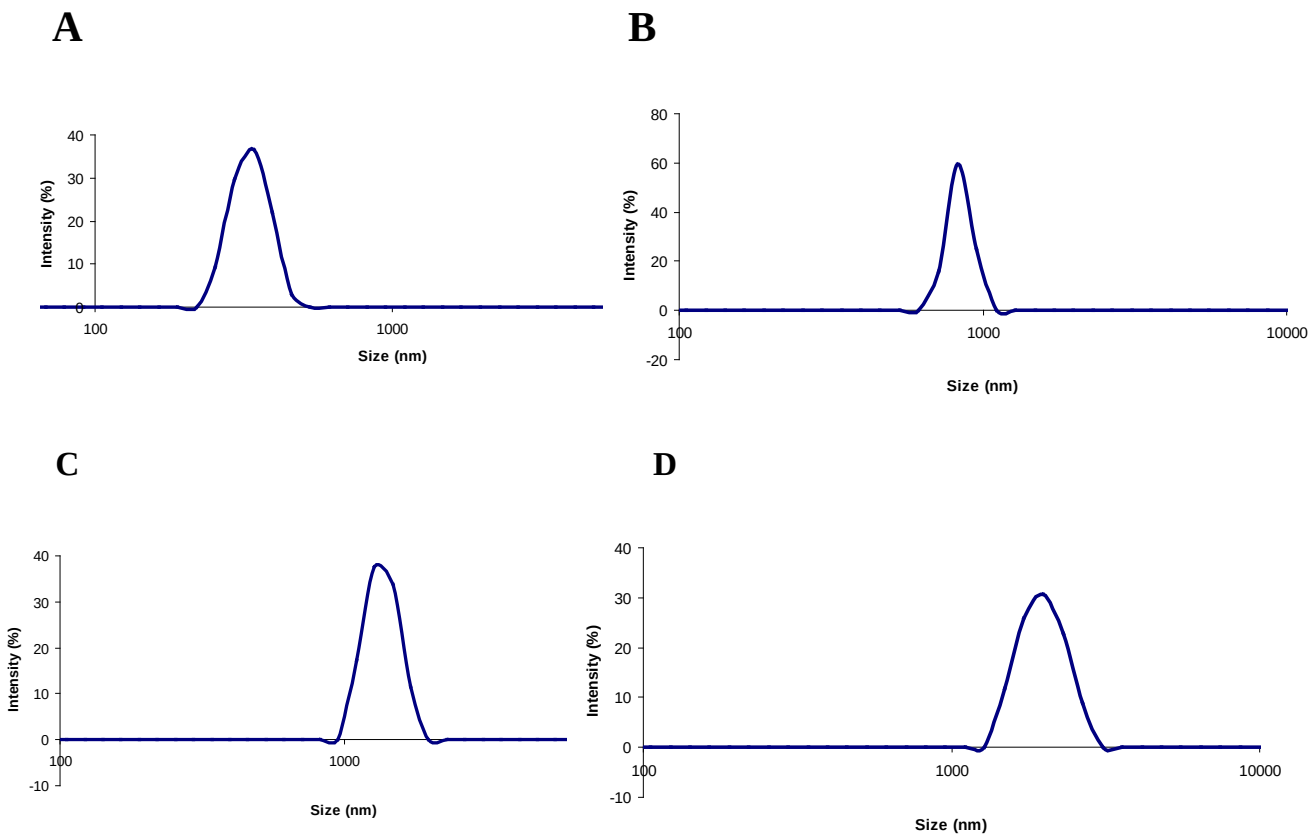

Figure 3.1. Z-averages of surfactant-free nZVI by Intensity measured by DLS. **A**. 0h. **B**. 1h. **C**. 2h.**D**.3h

To measure the rate of aggregation the size of the nZVI aggregates were plotted with respect to time. It was determined that particles start to aggregate right after synthesis in a linear correlation for three hours as can be seen in figure 3.1.

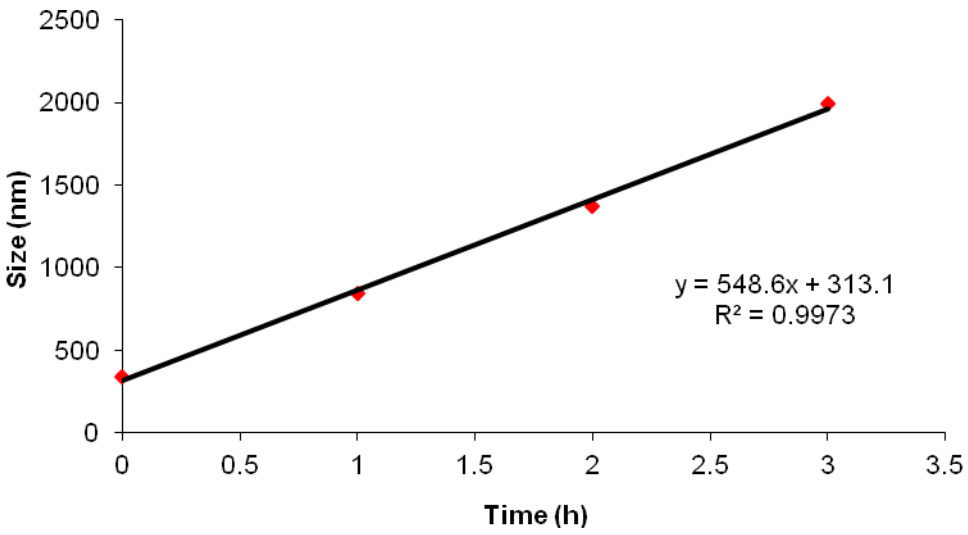

Figure 3.2 Z-averages of nZVI aggregates over time indicating that the rate of aggregation linearly increases for a three hour duration.

To determine maximum aggregation of nZVI, DLS measurements were taken over a longer duration of time (24 and 48 hours). This also indicated long term stability of the nZVI aggregates in solution which can be observed in figure 3.2.

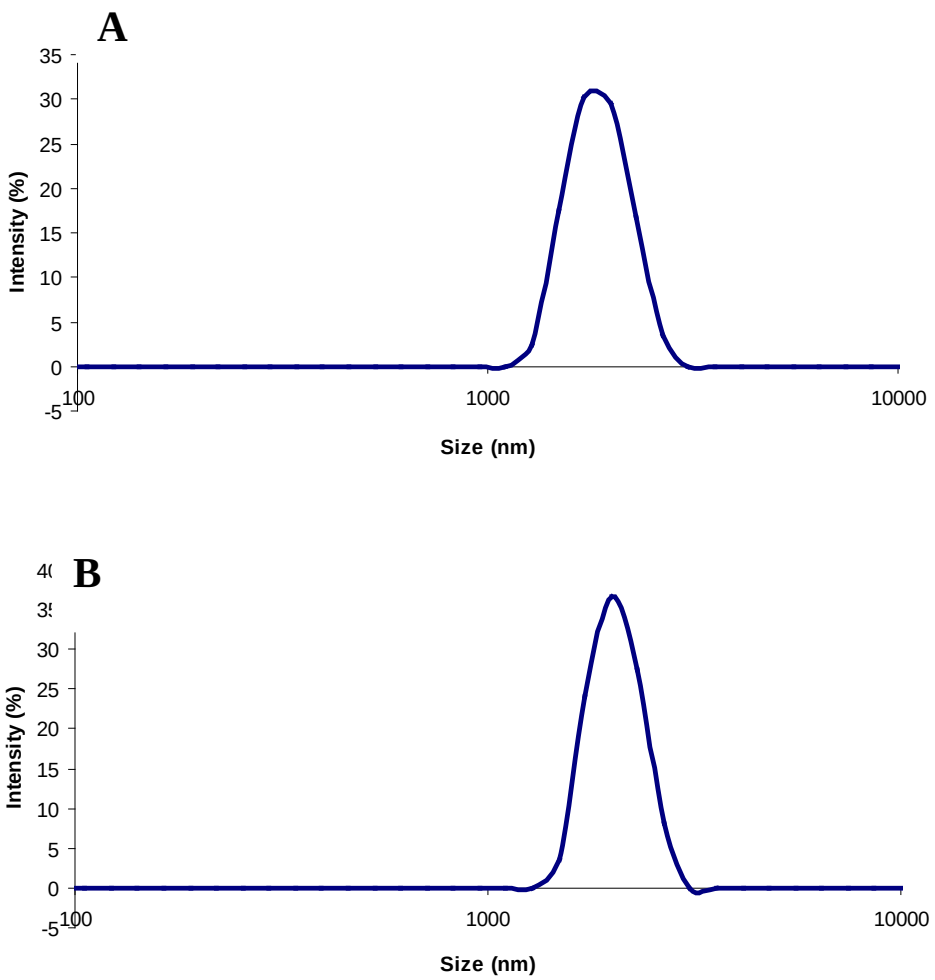

Figure 3.3 Z-averages of nZVI aggregates by Intensity by DLS. **A**. 24h. **B.** 48h.

3.1.2 Atomic Force Microscopy

Micrographs of 5µm x 5µm size were imaged of a four hour old nZVI sample. The purpose was to establish that nZVI quickly formed micro-sized aggregates in order to test DLS results. AFM is predominantly used to measure the height of nanoparticles but it can also provide a scale to indicate diameter examples of which are tabulated in table 3.2.

Table 3.2 Widths and heights of nZVI aggregates that have formed after 4 hours.

Field of View within a Sample	**Width (µm)**	**Height (nm)**
1	2.5	46.8
2	3.0	79.2
3	1.5	27.0
4	3.0	28.6

It was concluded that nZVI form micro sized aggregates, though their heights are relatively low and within the nano-scale due to the aggregates being flattened on the mica surface as shown in figure 3.4. Very few aggregates were present due to what appears to be the nanoparticles forming only a few but very large clusters. It was determined that the mean aggregate size three hours after synthesis was 2.5 (±0.7) µmwhich agrees with DLS data.

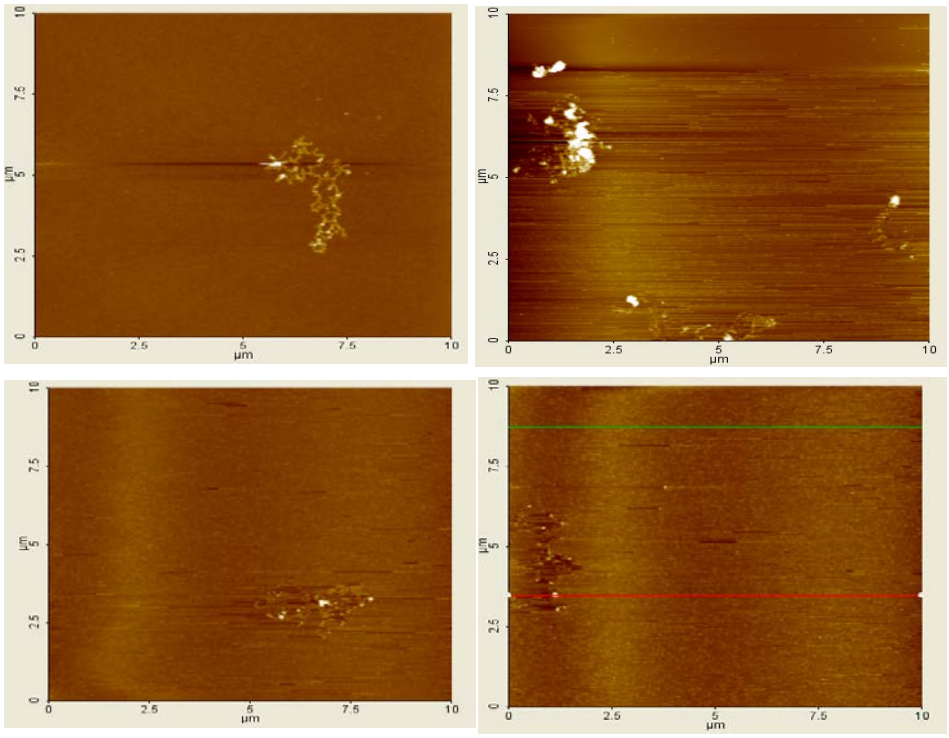

Figure 3.4 AFM images indicating that nZVI forms micro-sized aggregates

3.1.3 X-Ray Diffraction

X-Ray diffraction patterns were produced in order to determine the lattice structure of nZVI particles and to detect the presence of the various components in nZVI such as the zero valent iron core as well as the formation of an iron oxide shell. In addition, by obtaining the peak broadening of the peak specific to zero-valent iron using the XRD software, the size of the particle can be calculated and was determined to be 240 nm which was calculated using the Scherrer equation:

$$\tau = \frac{K\lambda}{\beta_{\tau} Cos\theta} \qquad \text{Equation 3.1}$$

The lattice structure for zero valent iron was cubic with unit cell dimensions a, b and c equalling 8.3A. The lattice structure for iron oxide was found to be tetragonal with unit cell dimensions a equalling 8.43A and c equalling 25.0A. Peaks for an nZVI sample were taken immediately after synthesis to indicate a definite presence of a zero valent iron core and very low intensity peaks for iron oxide and is shown in figure 3.5.

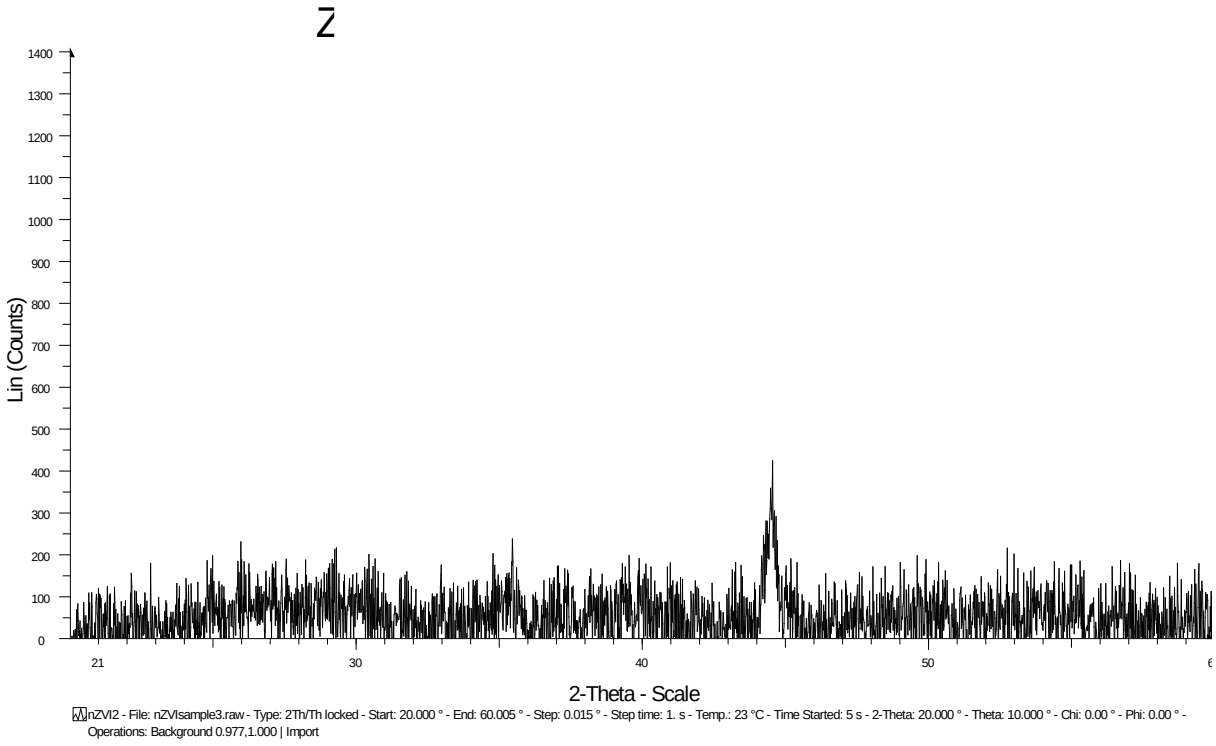

Figure 3.5 XRD phase plot of a fresh nZVI sample indicating the presence of a zero valent iron core at 45° and low intensity peaks at 30° and 35° indicating the absence of a large iron oxide shell.

3.1.4 Transmission Electron Microscopy

To reconfirm aggregation of nZVI without a surfactant with DLS, AFM and XRD results, TEM images were taken in order to establish the increase in size of nanoparticle aggregates at various time points of 0 hours and 24 hours which can be seen in figures 3.6 and 3.7. Fresh samples show nZVI aggregates ranging from 200-300 nm which agree with DLS, AFM and XRD results.

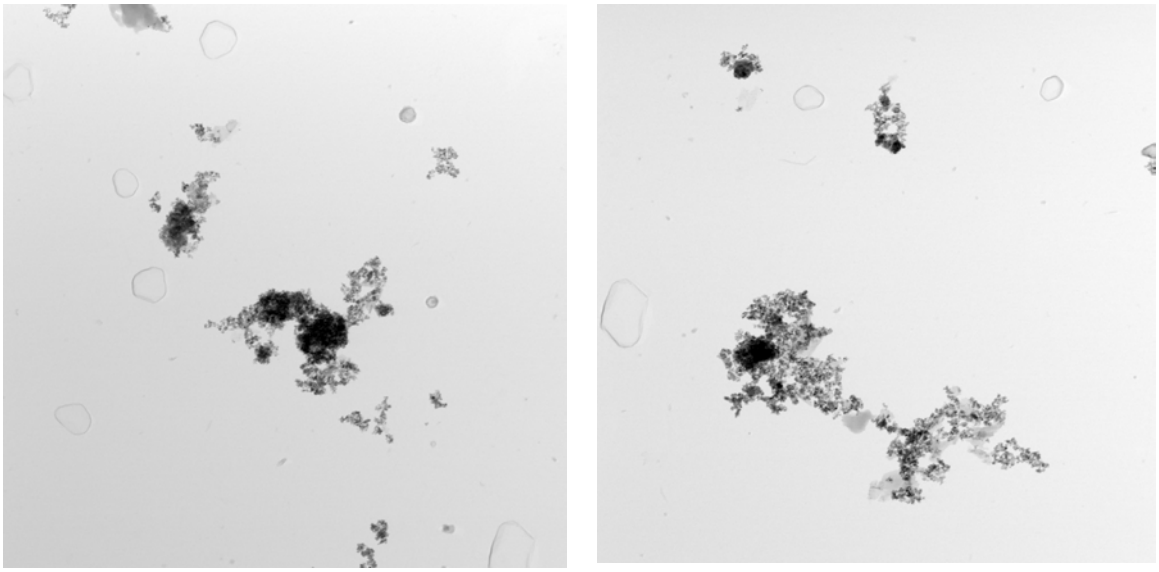

Figure 3.6 TEM images of fresh nZVI samples at 0 hours which showed to have aggregated to sizes ranging from 200-300 nm.

To assess the rate of aggregation, TEM images were also taken of a 24 hour aged sample in order to monitor the increase in size of the aggregates. Aggregates ranged from 2-3 μm which agrees with DLS and AFM results.

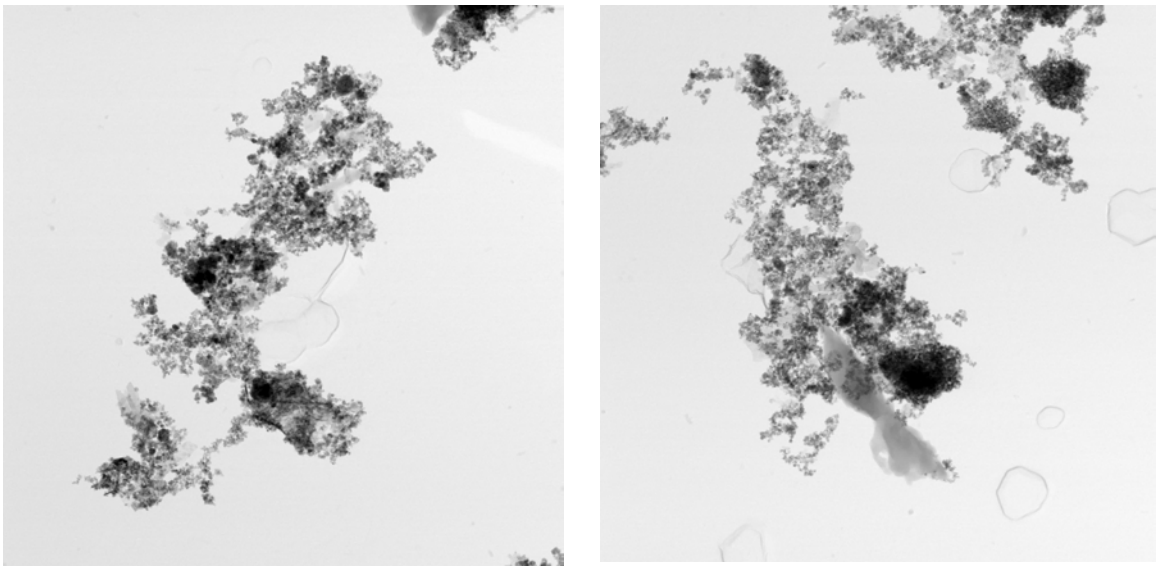

Figure 3.7 TEM images of aggregated nZVI after 24 hours resulting in aggregates ranging from 2-3 µm.

3.1.5 Zeta Potential

Zeta potential of the nanoparticle suspension was measured to determine the charge stability of the dispersed particles in solution at different pHs. It was determined that as the pH increased to become more alkaline, the zeta potential of the nanoparticles decreased. The iso-electric point of the nanoparticles was found to be 8.1 as seen in figure 3.8 where the surface charge is 0 and is the point of maximum aggregation.

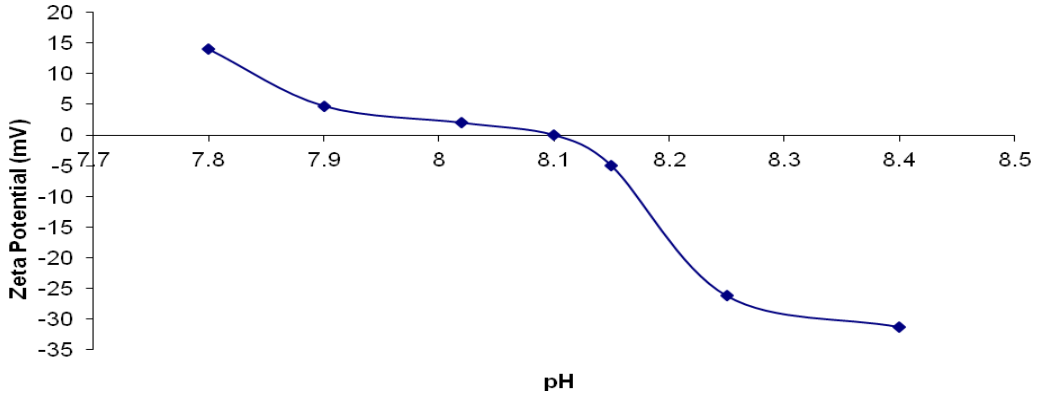

Figure 3.8 Change in zeta-potential by altering the pH of the nanoparticle suspension.

3.1.6 UV-Vis Spectroscopy

UV-Vis was taken of a sample immediately after synthesis in order to further characterize and determine the absorbance maxima of nZVI. The purpose of this was to determine the presence of nZVI based on the known nZVI peak in literature. The nZVI absorption maxima was determined to be 230 nm indicating the definite existence of nZVI in the sample and can be seen in figure 3.9.

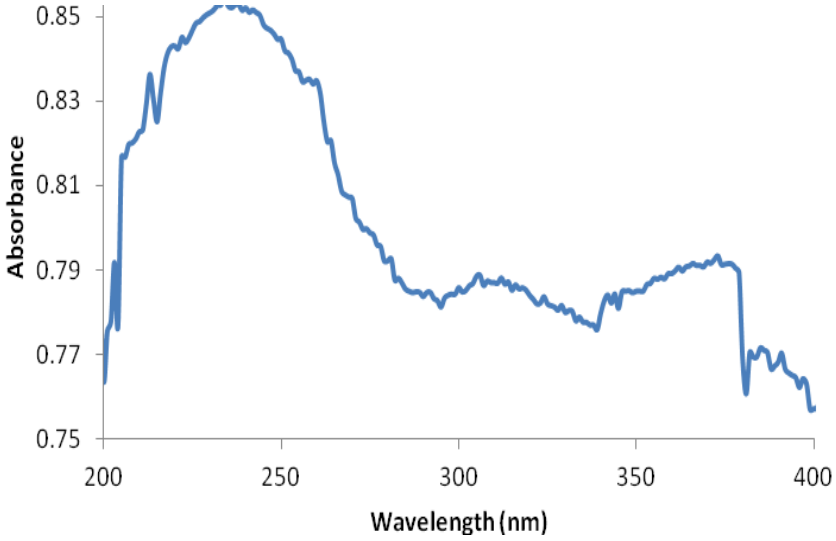

Figure 3.9 UV-Vis absorption spectra of nZVI indicating the presence of nZVI with an absorption maxima at 230 nm.

3.2 Rhamnolipid Surfactant Effect on Zero Valent Iron Nanoparticles

3.2.1 Dynamic Light Scattering

The hydrodynamic diameter of nZVI that were capped with the rhamnolipid surfactant were measured by DLS at different time points. The purpose of this was to assess rhamnolipid's effect on the dispersion of the nanoparticles and to establish if the surfactant was able to limit the aggregation of the nanoparticles. Particles with nano dimensions were then filtered to separate the larger nZVI aggregates to obtain a sample of rhamnolipid dispersed nZVI as seen in figure 3.3.

Table 3.3 Hydrodynamic Diameters of nZVI aggregates over a three hour period. Diameters are Z averages of five measurements

Time (h)	Hydrodynamic Diameter (nm)	Polydispersity Index
0	122 ± 0.21	0.224
1	132 ± 0.34	0.515
2	142 ± 0.45	0.274
3	165 ± 0.38	0.492

The rate of aggregation of nZVI was calculated based on DLS results over a 4 hour time period in order to assess rhamnolipid's efficiency at being able to disperse nZVI. Particles that were incorporated with rhamnolipid surfactant showed to have a very low aggregation rate and maintained a small size just over 100 nm seen in figure 3.10 in comparison to particles without a surfactant that quickly aggregated to over a micron in size. Rhamnolipid alone was measured by DLS though had a very low count rate.

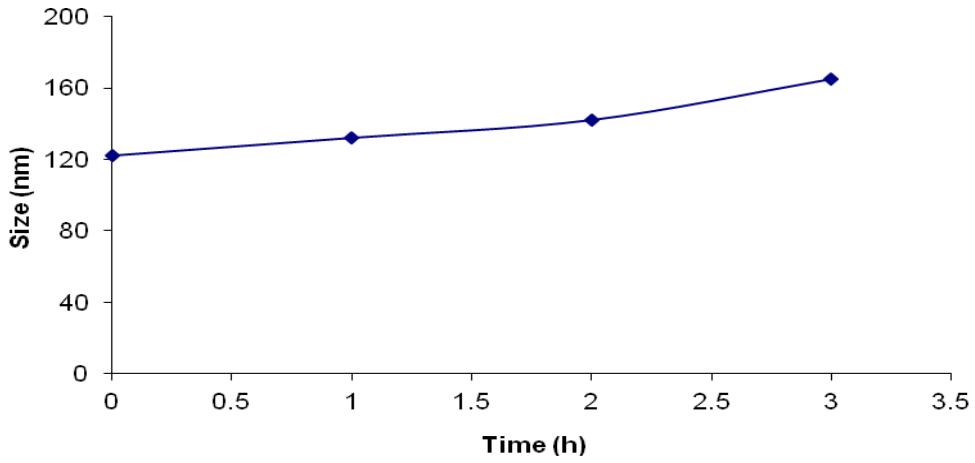

Figure 3.10 Size of rhamnolipid incorporated nZVI over a three hour time period indicating that rhannolipid is able to limit aggregation of nanoparticles so that particles are able to retain nano size.

3.2.2 Atomic Force Microscopy

Arbitrary 5µm x 5µm sections of AFM micrographs were taken of the nZVI sample on the mica slip. This was done to obtain images of the nZVI particles and to quantify a size of the particles based on height. Over 100 nZVI particle heights were taken to obtain an accurate distribution of size. The average height and width for the nanoparticles was found to be 50 nm seen in figure 3.11.

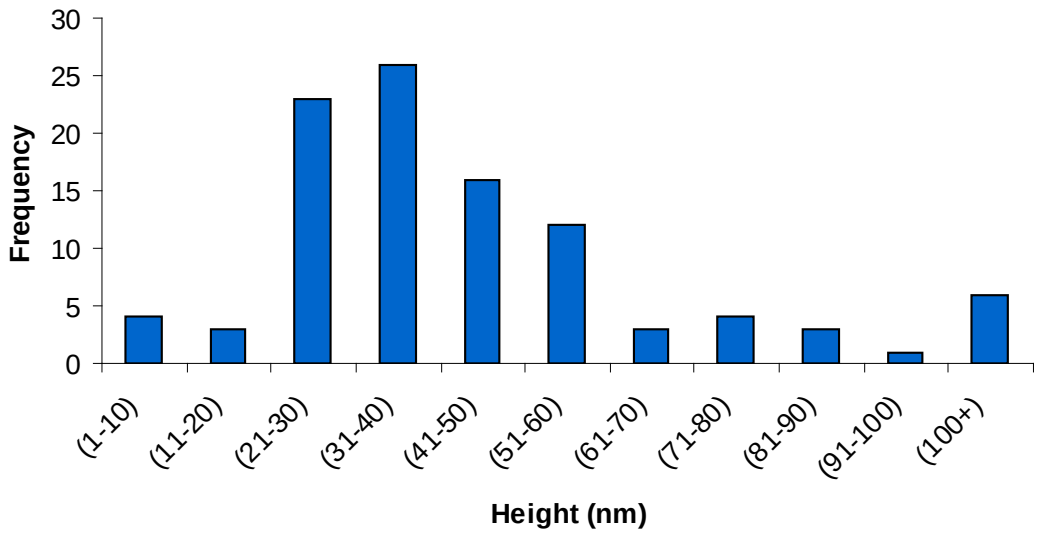

Figure 3.11 Height comparison of nZVI by AFM measurement.

3.2.3 X-Ray Diffraction

X-Ray diffraction patterns were created in order to determine the lattice crystal structure of the nZVI core as well as the iron oxide shell. By determining the peak broadening from the diffraction pattern using the XRD software, the size of the nanoparticle can be calculated. The lattice system for Iron was found to be cubic having unit cell dimensions of a/b/c= 2.865A. The

lattice system for Fe_2O_3 was found to be tetragonal with unit cell dimensions of a/b=8.43A and c=25.02. The size of the nZVI nanoparaticle was determined to be 76.4 nm. Peaks indicating the presence of zero valent iron and iron oxide can be seen in figure 3.12.

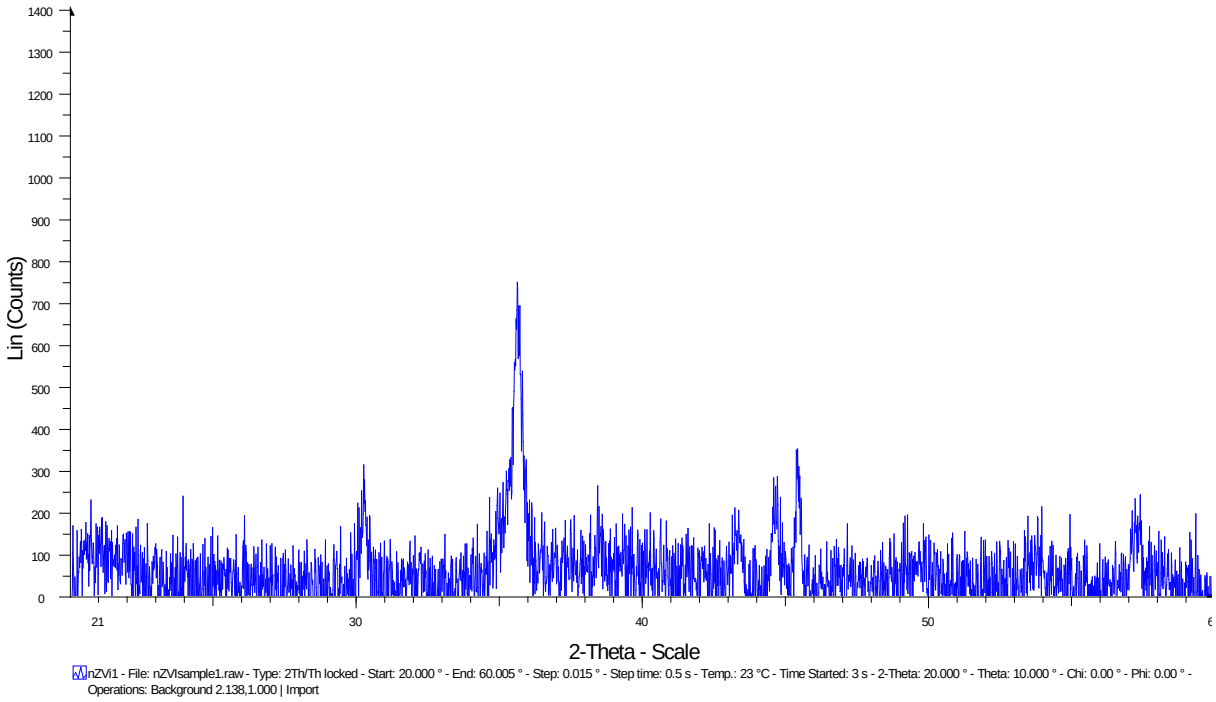

Figure 3.12 XRD phase plot of an aged (48 hours) nZVI sample indicating high intensity peaks at 30°, 35° and just below 45° indicating the presence of an iron oxide shell. A peak at 45° indicates the presence of zero valent iron.

3.3 Reduction of Cr(VI) to Cr(III) by aggregated micron sized nZVI

3.3.1 Flame Atomic Adsorption Spectroscopy

The final goal of this study was to separate physically the free Cr(VI) and iron bound Cr(III) which is usually difficult with nano sized material. FAA was used to determine the concentration of Cr(VI) present after exposure to micron sized aggregates that were formed from nZVI. Cr(VI) that had been reduced to Cr(III) by the micron sized aggregates would have solidified and as well as formed a complex with iron and therefore could be centrifuged into a pellet and can be separated from solution phase Cr(VI). FAA was taken to measure the concentration of the Cr(VI) which was left in the supernatant. The purpose of this was to determine the decrease in concentration of solution phase Cr(VI) due to the conversion of Cr(VI) to Cr(III) by iron. It was concluded that 1 gram of micron sized ZVI was able to reduce 3 mg of Cr(VI) to Cr(III) in 4 hours and can be seen in figure 3.13.

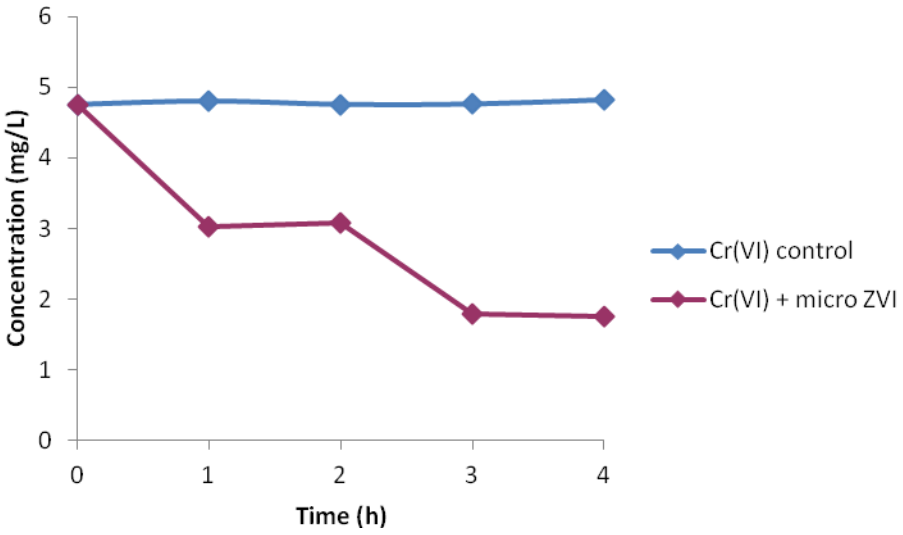

Figure 3.13 Decrease in the concentration of Cr(VI) after exposure to 1 gram of aggregated micron sized nZVI.

3.3.2 Rate of Reaction

Concentration results from FAA were used to calculate the rate order of reaction for the reduction of Cr(VI) by micro sized ZVI. The purpose of this was to determine the reaction kinetics of the reduction of Cr(VI). It was concluded that Cr(VI) removal by micro sized ZVI followed a second order rate equation which can be seen tabulated in table 3.4.

Table 3.4 Concentration of Cr(VI) with respect to time with respect to second order reaction kinetics

Time (h)	**1/C**	**$1/C_0$**
0	0.211	0.211
1	.330	0.211
2	0.325	0.211
3	0.559	0.211
4	0.573	0.211

It was determined that the reduction of Cr(VI) to Cr(III) by aggregated micro size nZVI was a second order reaction indicating that the reaction is dependent on the concentration of the reactant. The line of best fit which exemplifies second order reaction kinetics has an R^2 value of 0.96 and can be seen in figure 3.14.

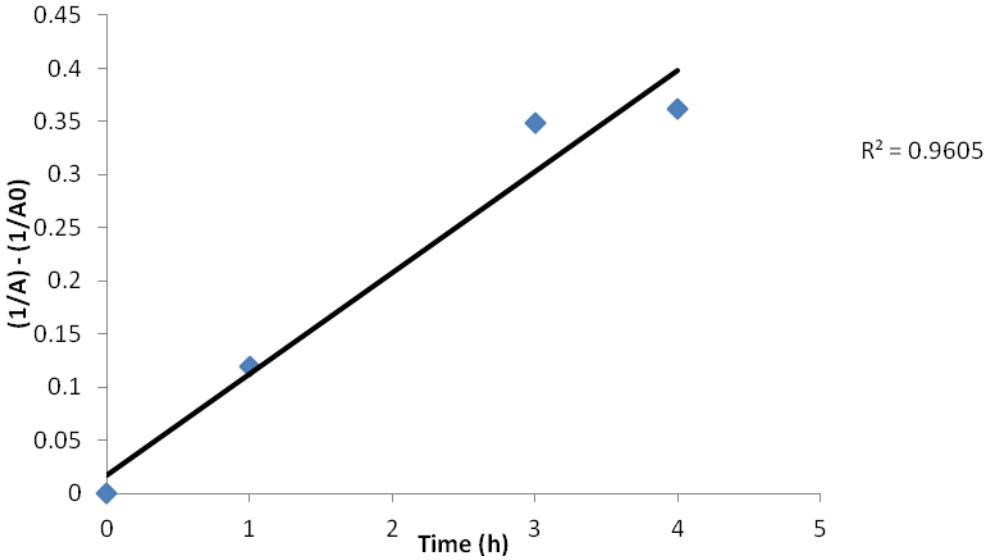

Figure 3.14 Reduction of Cr(VI) follows second order reaction kinetics which can be seen in a linear slope between initial and final concentration with respect to time.

3.4 Reduction of Cr(VI) to Cr(III) by nZVI

3.4.1 Flame Atomic Adsorption Spectroscopy (FAAS)

FAAS was used to determine the concentration of Cr(VI) after exposure to nZVI. After reduction of Cr(VI) by nZVI, Cr(III) binds to iron and therefore can be centrifuged into a pellet which decreases the concentration of solution phase Cr(VI) whereby the concentration of the remaining Cr(VI) in the supernatant can be measured by FAAS. The purpose of this was to determine the efficiency at which nZVI is able to reduce the oxidation state of Cr(VI) to Cr(III) as well as to measure the decrease in solution phase chromium. It was determined by FAAS results that 1 gram of nZVI is able to reduce 36 mg of Cr(VI) to Cr(III) which can be seen in figure 3.15.

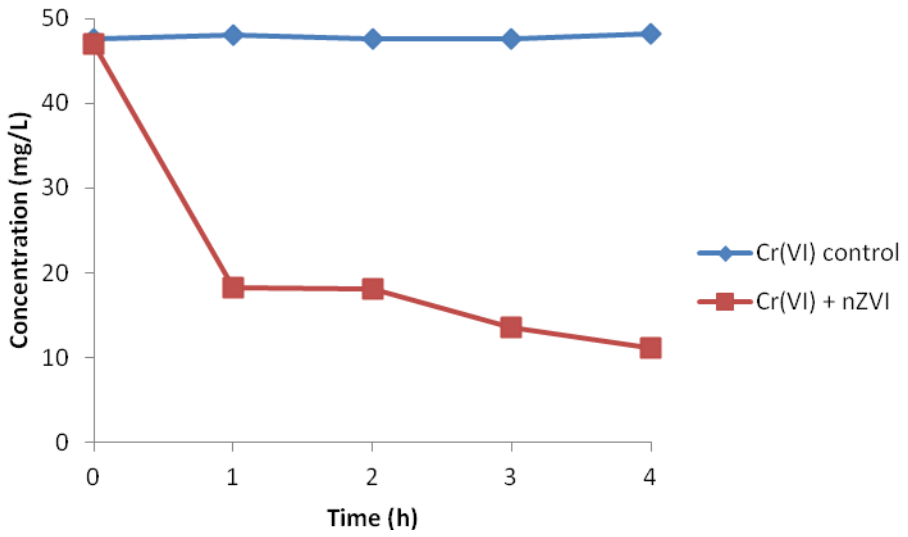

Figure 3.15 Decrease in solution phase Cr(VI) concentration after exposure to 1 gram of nZVI

3.4.2 Rate of Reaction

FAAS concentration results were used to determine the rate order of reaction for the reduction of Cr(VI) by nZVI. This was done to obtain the rate order constant for the kinetics for the reduction of Cr(VI) by nZVI. It was determined that this process was a first order reaction which compared the concentration of Cr(VI) with the original concentration with respect to time which is tabulated in table 3.5.

Table 3.5 Concentration of Cr(VI) with respect to time follows pseudo first order kinetics

Time (h)	**Ln($C/C_{0)}$**
0	0
1	-0.945
2	-0.952
3	-1.238
4	-1.433

The reduction of Cr(VI) to Cr(III) by nZVI was established to be a pseudo first order rate of reaction in which the trend line has an R^2 value of 0.97 which can be seen in figure 3.16.

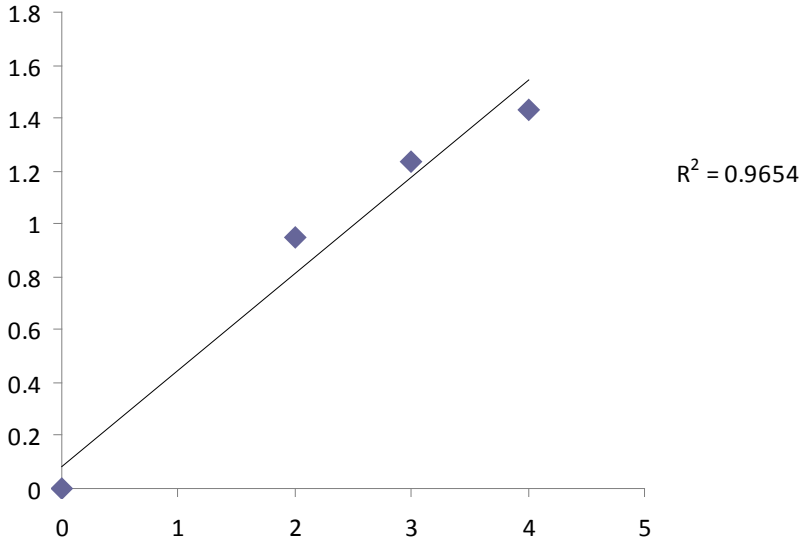

Figure 3.16 Reduction of Cr(VI) by nZVI appears to have a pseudo first order reaction which can be seen with a linear slope of concentration with respect to time.

Flame atomic adsorption results allow a comparison to be made between the effectiveness of reduction of Cr(VI) to Cr(III) using 1 gram of micro scale ZVI versus 1 gram of nZVI. The purpose of this is to prove that nZVI is more efficient and able to reduce a larger amount of Cr(VI) to Cr(III) compared to micro scale ZVI. It was proven that nZVI was able to reduce approximately ten fold greater amount of Cr(VI) compared to micro scale ZVI in a time scale of 4 hours which is given in table 3.6.

Time	**Reduced Cr(VI) by micro scale ZVI (mg)**	**Reduced Cr(VI) by nZVI (mg)**
1	1.721	28.73
2	1.675	28.85
3	2.961	33.37
4	3.003	35.78

Table 3.6 Comparison between the amounts of Cr(VI) reduction using either 1 gram of micro scale ZVI or 1 gram of nZVI. It is determined that nZVI is about 12 fold more efficient at reducing Cr(VI) at 4 hours.

4.0 Discussion

4.1 Aggregation of zero valent iron nanoparticles without surfactant

It was determined that uncapped nZVI nanoparticles aggregate rapidly after synthesis to form micron sized aggregates that remain stable in solution over an extended length of time of 48 hours. Three separate methods of DLS, XRD and AFM were used to determine the size of nZVI particles in order to establish aggregation rate of the nanoparticles without the use of a surfactant. DLS results demonstrated that at a particle concentration of 5g/L particles do not remain dispersed. DLS measurements were taken immediately after synthesis of a fresh nZVI sample which showed aggregate sizes at approximately 300 nm indicating that nZVI particles start to amass during and after synthesis. Particles aggregate for three hours and aggregates reach micron size. After three hours, the size of the particle aggregates remains at a constant size indicating stability of the micron size ZVI aggregates in solution for an extended amount of time of 48 h. These findings can be explained by the laws of Brownian motion which state that dispersed colloidal particles which are smaller than 5 μm are affected by Brownian motion in a medium. The collisions between particles cause the particles to aggregate and cause the creation of large particle aggregates which are able to sediment out of solution (Kelkar et al, 2012). In an attempt to reduce this effect, a biological rhamnolipid surfactant was incorporated in order to stabilise the nanoparticles and comparison results will be discussed.

XRD phase plot results confirm aggregation of nZVI nanoparticles without the presence of a surfactant. An XRD phase plot was taken of nZVI immediately after synthesis which shows low intensity peaks indicative of the presence of iron oxide as well as a clear peak at 45° indicative of the presence of nZVI. The size of the nZVI particles was calculated using the Scherrer equation

and found to be 240 nm indicating that without the incorporation of a surfactant, particles started to aggregate immediately after synthesis which agrees with DLS results. The phase plot results qualitatively show that the intensity of the nZVI peak was relatively high indicating that the majority of particles existed as nZVI and a minority as iron oxide. This could be due to fresh nanoparticles not having been exposed to air so that they had not been oxidized. XRD results indicate that the nanoparticles crystal structure is cubic for zero valent iron with unit cell dimensions a/b/c equalling 8.3A and the lattice system for iron oxide was determined to be tetragonal with unit cell dimensions a/b equalling 8.4A and c equalling 25.0A. When comparing the obtained XRD phase plot to an XRD phase plot of an aged sample conducted by Zhang and Elliot, 2006, it can be seen that the peak for nZVI decreases in intensity due to the oxidation of the zero valent iron and simultaneously the iron oxide peak increases in intensity.

AFM reconfirms DLS and XRD data and shows nZVI quickly aggregate to form micron sized clusters. Four hour old nZVI samples showed to have aggregated into clusters ranging from 1.5-3 µm. AFM is mainly used to measure the height of particles though AFM micrographs show many nZVI aggregates possessing diameters in the micron range and having heights of nano-dimensions indicating that the aggregates are flattened on the mica substrate. Nano sized particles aggregated to create few but large micron sized aggregates which is why many clusters were not observed in the AFM micrographs.

TEM images reconfirm DLS and AFM results indicating that surfactant free nZVI quickly aggregate. TEM images of a fresh nZVI sample taken at 0 hours show to have clusters of nZVI particles ranging from 200 nm which indicate that nZVI samples do not remain dispersed nor

retain a nano size and start to form clusters immediately. A 24 hour aged sample of nZVI shows to have created large aggregates in the micro size ranging from 2-3 µm. Nanoparticles are not able to remain dispersed and forms large clusters, which leads to a smaller specific surface area of the particles being exposed to the surroundings. In cases of environmental remediation where nZVI is used to interact with hazardous chemicals, a high specific surface area must be available to increase the efficiency of reactions. Better dispersion of nZVI can be done using a surfactant which would lead to nanoparticles not aggregating and therefore staying in the nano range and exposing a high specific surface area to react with chemicals.

4.2 Nanoparticle Aggregation and Surface Charge

The results focusing on the zeta potential of nZVI strongly suggest that pH impacts zeta potential. Results show that as the pH increases and becomes more alkali, the zeta potential becomes more negative due to nZVI particles obtaining a negative charge. The isoelectric point (IEP) was determined to be 8.1 and is the pH at which the nZVI have a neutral charge and therefore a zeta potential of zero. Considering that the particles have a neutral charge, there are no repulsive forces between particles and therefore the IEP also represents the point of highest aggregation and therefore highest instability of particles. The decreased dispersion of nZVI will lead to a smaller specific surface area of the particles being available to interact with toxic chemicals such as Cr(VI) and therefore decrease the amount of Cr(VI) being converted into less harmful Cr(III). Aggregation will also ultimately impact the nanoparticles ability to remain suspended in solution which also impacts their mobility in environmental waters. The incorporation of a rhamnolipid surfactant would act as a stabilizer which would have provided steric hindrance by electrostatic interactions around the particles and thereby decreasing aggregation (Xie et al, 2006).

Other studies also examine aggregation of nZVI due to pH using commercially available nZVI. Commercially available nZVI possessed a much lower IEP of approximately 6 (Yin et al, 2012) in comparison to the laboratory synthesized nZVI created in this study which has an IEP of 8.1. This can be explained as at a pH of 7 the commercial nZVI showed to possess a negative charge in comparison to the nZVI synthesized in the laboratory in this study showed to have a positive charge. The lower IEP shown by commercial nZVI is actually more representative of iron oxide which could be formed due to nZVI contact with air in the packaging or due to the nZVI becoming older during the process of shipping and could decrease the efficiency of its ability to donate electrons (Lee and Sedlack, 2008). The purpose of this project was to convert Cr(VI) to Cr(III) using nZVI, which would change the oxidation state of Cr(VI) by nZVI donating electrons. Obtaining commercially available nZVI may not be as reliable due to the fact that the nanoparticles are exposed to oxygen for an extended duration of time allowing them to rapidly oxidize so that any experiments conducted on the aggregation of commercial nZVI is actually more representative of iron oxide. The nZVI that were created in this project were covered in a layer of ethanol for storage to prevent oxidation until use. This current study is a more accurate representation of the change in zeta potential with respect to pH due to the fact that the particle being measured is definitely nZVI and not iron oxide which can be seen in the change in the IEP.

4.3 Aggregation of surfactant protected zero valent iron nanoparticle

Results demonstrate that rhamnolipid surfactant is able to disperse nZVI so that particles remain in the nano-sized range and do not aggregate over an extended duration of time. DLS, XRD and AFM were the three techniques used to determine the size of nZVI particle that had been

synthesized with the incorporation of rhamnolipid surfactant. DLS results indicate that the surfactant is able to disperse a certain portion of particles so that particle size is approximately 120 nm compared to 371 nm which was the particle size without the use of a surfactant. The results also show that the rhamnolipid is able to prevent aggregation of the particles over an extended time compared to particles that were not synthesized with the surfactant which aggregated to micron size range. Results show that rhamnolipid surfactant was only able to disperse a certain portion of particles as nZVI and a portion of particle still managed to aggregate though the nano-sized particles could be easily separated from the portion of larger aggregates using filter paper.

In comparison to other studies conducted such as the work presented by Dong and Lo, (2012), it can be observed that rhamnolipid surfactant is more effective at dispersing nZVI and creating smaller sized nZVI. Surfactants Tween-20 and Starch were chosen to investigate the surfactants ability to reduce aggregation of nZVI (Dong and Lo, 2012). Tween-20 showed an ability to maintain stability of nZVI for 6 hours of approximately 180 nm by DLS though rhamnolipid indicated to be a superior surfactant as it was also able to maintain the size stability of nZVI but at a much lower particle size of approximately 120 nm by DLS. Starch was also used as a surfactant in an attempt to stabilise nZVI particle size and showed to limit the rate of aggregation and keep particle size constant at approximately 350 nm. Though the starch surfactant was indeed able to reduce aggregation, in comparison, rhamnolipid was able to keep particle size much smaller at 120 nm which is approximately half the size of the particles that were dispersed by starch. Starch is a hydrophilic polymer comprising of glucose molecules while rhamnolipid is amphiphillic possessing both hydrophilic and hydrophobic regions. Tween-20 is a non-ionic

surfactant while the carboxylic acid group on rhamnolipid possesses a negative charge which adds to the usefulness of rhamnolipid as a surfactant by providing repulsive forces. The combined effect of rhamnolipid being both ampiphillic and anionic is what contributes to smaller sized nZVI particles being created as well as limited aggregation of nZVI particles.

XRD results confirm that rhamnolipid is able to lessen the aggregation of nZVI so that particles remain dispersed in a nano-sized range. XRD phase plots for a rhamnolipid surfactant incorporated nZVI aged sample show defined peaks for iron oxide as well as a definite and distinct peak at 45° indicative of the presence of nZVI. The particle crystal size of an aged sample of 48 h had a defined peak indicating the definite presence of nZVI and represented a particle size of 76.6 nm ensuring that particle size was able to remain in the nano scale over an extended duration of time confirming that there was limited aggregation of the nanoparticles. The long term dispersion of nZVI can be attributed to the inclusion of the rhamnolipid surfactant.

AFM results further confirm that rhamnolipid is able to disperse nZVI particles and maintain their nano-size by ensuring colloid stability. Examination of the AFM micrographs shows that the majority of the nZVI particles had a height between 20-60 nm with an average particle size of 50 nm which is consistent with the results from other size measuring techniques. These results indicate that with the incorporation of a surfactant, nZVI is able to remain properly dispersed so that the particles exist in their nano size. The minority of aggregates that had formed had sizes smaller than those determined by DLS probably due to aggregates having lower dimensions in terms of height ultimately resulting in a lower size detected by the AFM. AFM micrographs of nZVI samples of an older sample show that the nZVI particles still exist in their nano form which

shows that long term dispersion of nZVI is highly dependent on a surfactant so that the attractive forces between nZVI particles are overcome.

Dispersion of nZVI happens due to rhamnolipid being able to stabilize the nanoparticles by providing steric hindrance around the particles which is dude to electrostatic interactions between the negative charges on the rhamnolipid. Since rhamnolipid allows for nanoparticles to retain their nano dimensions without aggregating, this results in smaller sized particles which have a high specific surface area. The large surface allows for a larger area to react with Cr(VI) resulting in more Cr(VI) being converted to Cr(III). The Cr(III) binds to iron and makes a solid iron-chromium complex which can be removed resulting in a decrease of solution phase chromium. This provides an excellent means of removing toxic Cr(VI) that exists in environmental water.

4.4 Zero valent iron nanoparticle size distribution

When comparing the sizes of the nanoparticles and aggregates, there appears to be a discrepancy between the sizes obtained by the various methods, which is attributed to the type of technique used. The hydrodynamic diameter acquired by DLS appeared to be larger than the sizes attained by other methods. A possible reason for this could be due to the high concentration (5 g/L) of nZVI used in DLS samples. The reason a higher concentration was chosen was to keep the mass of nZVI used consistent with different techniques. XRD analysis requires the sample to be in powder form and a minimum of 5-10 grams is needed to properly fill the sample holder. The same concentration range was kept consistent for AFM samples.

The size distributions were decreased with the incorporation of the rhamnolipid surfactant due to the surfactants hydrophobic properties, which created micelles and therefore able to disperse the nanoparticles. The rhamnolipid surfactant was chosen in this study over other chemical based surfactants as rhamnolipid is more biodegradable and less toxic to the environment.

When comparing the size of particles and aggregates, three different methods of DLS, XRD and AFM were used. The sizes provided by each of these methods were consistent between XRD, AFM and DLS though DLS was slightly higher. This is due to DLS measuring the hydrodynamic diameter of particles which includes a hydrated shell around the particle and is measured as part of the particle and therefore will give a higher size value. XRD gives the size of the lattice structure and AFM gives the height of the particle.

UV-vis results confirm the presence of nZVI in a sample suspended in DI water where the nanoparticles showed their absorption maxima at 230 nm which agrees with literature results (Singh et al, 2011). After reaction with Cr(VI), the nZVI is oxidized and forms a complex with Cr(III). Compared to other research by Salaun and Salaun, (2007), UV analysis of the chromium would indicate an alternate UV peak at 371 which is designated to the presence of chromium which would confirm that nZVI donates electrons to Cr(VI) and in turn becomes oxidized. The presence of a chromium peak would also confirm that nZVI reduces Cr(VI) into Cr(III) and simultaneously the nZVI is oxidized into Fe(III) which co-precipitates with Cr(III) and is captured in the pellet. This is useful information as not only is Cr(VI) converted into a less toxic form but the co-precipitation renders chromium to be immobile, making it less of a hazard in the ecosystem.

4.5 Reduction of Cr(VI) to Cr(III) by aggregated nZVI which form micro scale ZVI

Atomic adsorption results exemplify that aggregated micro sized nZVI are quickly and effectively able to convert low amounts of Cr(VI) to Cr(III) by lowering the oxidation state which decreases the concentration of solution phase chromium. Atomic adsorption results demonstrate that the concentration of the control consisting of only Cr(VI) remains consistent. This confirms that without any other parameters involved, the concentration of Cr(VI) is not affected. By changing one external factor such as the addition of aggregated micro sized nZVI particles, the change in concentration of Cr(VI) is specifically due to the changes induced by the nanoparticles.

Results show that with the addition of 1 gram of micro ZVI particles, the original concentration of 5 mg/L of Cr(VI) decreases to approximately 3 mg in one hour confirming that micro scale ZVI is capable of converting solution phase Cr(VI) to Cr(III) which forms a complex with iron and can be separated from the remaining solution phase Cr(VI). Atomic adsorption results reveal that over a three hour time period, micro scale ZVI is able to reduce approximately three grams of Cr(VI) into Cr(III). This is due to ZVI being a reducing agent and therefore donating electrons to Cr(VI). Though results confirm that aggregated nZVI which forms micro scale ZVI aggregates, is indeed able to reduce Cr(VI), the micro scale ZVI is still limited by its large size and therefore smaller specific surface area. Specific surface area of a sphere shaped particle can be calculated using the equation below:

$$SSA = \frac{Surface\ Area}{Mass} = \frac{\pi d^2}{\rho \frac{\pi}{6} d^3}$$ Equation 4.1

The density of iron (ρ) is known to be 7800 kg/m^3 and the diameter of a micro scale ZVI is taken from the DLS results at 3 hours resulting in a particle with a diameter of 1993 nm. The specific surface area of a micro scale ZVI spherical aggregate is 386 m^2/kg. By decreasing the size and diameter of the particle, the specific surface area will contingently increase and thereby give a larger surface to react with the Cr(VI).

Other studies focus on the removal of Cr(VI) by micro scale ZVI suggest that under 7% of Cr(VI) was removed by ZVI and iron oxide micro particles of 10µm (Alidokht et al, 2011). In comparison, removal of solution phase Cr(VI) by a change in oxidation state to Cr(III) with ZVI microparticles used in this project had a reduction efficiency of 63%. This is due to the fact that the microparticles used in this project were aggregates of nZVI particles and had a maximum aggregation size of 2000 nm as determined by DLS which is significantly smaller than the 10 µm microparticles used in the study performed by Alidokht et al, 2011. The more efficient conversion of Cr(VI) to Cr(III) by the micro particles aggregates used in this project were due to the fact that they are a smaller size and therefore possess a larger specific surface area to react with the Cr(VI) and therefore are able to reduce Cr(VI) more effectively. This indicates that even without a surfactant to stabilized and reduce the size of the nZVI aggregates, the microparticles created by the aggregation of nZVI particles are still more effective at reducing Cr(VI) compared to commercial micron sized NZVI particles as the aggregates created in this study are a smaller size compared to commercially purchased micron sized aggregates. This gives extreme promise that smaller particles that are stabilized by a surfactant will have an even greater efficiency at Cr(VI) reduction based on available specific surface area.

Results from this project can be compared to those conducted by Liu and Wei, (2012) where they stated that untreated nZVI was not able to reduce Cr(VI) even after extended exposure of up to 2.5 hours. This is mainly due to the oxidation of nZVI formed on the surface of the particles which inhibits any redox reactions from occurring with Cr(VI). Oxidation of nZVI was prevented in this project as nZVI particles were kept submerged in a layer of ethanol after synthesis in order to preserve the oxidation state. This prevention of oxidation allowed the particles to retain their oxidation state to be more efficient in changing the oxidation state of Cr(VI) to Cr(III). A second point to consider is that untreated nZVI particles were washed with acid in order to reduce them and were subsequently exposed to Cr(VI) several times (Lui and Wei, 2012). With each subsequent use of nZVI the rate of reduction of Cr(VI) was even less due to nZVI becoming oxidized. This decrease in efficiency could be due to the fact that nZVI was re-reduced with acid and therefore could still be partially oxidized and therefore would not have the heightened reducing power as nZVI synthesized in the current project.

4.6 Reduction of Cr(VI) to Cr(III) with rhamnolipid stabilized nZVI

It was shown that 1 gram of aggregated micro scale ZVI was able to convert approximately three grams of solution phase Cr(VI) to a lower oxidation state Cr(III). Since the detection limit for chromium was 5 mg/L and aggregated micro scale nZVI was able to convert 3 mg of Cr(VI), it was decided to expose only 0.1 of nZVI to 5 grams of Cr(VI). Atomic adsorption results show that in the first hour of exposure, 0.1 g of nZVI was able to reduce 2.87 of Cr(VI) after one hour of exposure. To make a direct comparison between nZVI and aggregated micro scale nZVI, one gram of micro scale ZVI was able to convert 1.7 grams of Cr(VI) to Cr(III) while 1 gram of nano scale ZVI is able to convert 28.7 grams. Results indicate that nZVI is 17 fold more efficient at

reducing Cr(VI) compared to micro scale ZVI in the first hour of exposure. Over a three hour time duration, 0.1 g of nZVI was ultimately able to convert 3.58 g of Cr(VI) by a process of changing the oxidation state. To compare the final Cr(VI) reduction by both forms of zero valent iron, in three hours micro scale ZVI was able to reduce 3 grams of Cr(VI) to Cr(III) whilst 1 gram of nZVI was able to reduce 35.8 grams of Cr(VI). Results indicate that nZVI is 12 fold more efficient at reducing Cr(VI) which can be attributed to the much higher specific surface area provided by nZVI compared to micro scale ZVI. The specific surface area of nZVI can be calculated to be 10,121 kg/m^2. The calculated results show that nZVI provides a 26 fold higher specific area for reaction with Cr(VI) compared to micro scale ZVI. These results demonstrate that very low concentrations of nZVI can be used to reduce substantial amounts of Cr(VI) which is economical and cost efficient.

Results from atomic adsorption indicate that the rhamnolipid surfactant was able to disperse the nZVI particles so that they were able to remain in a nano state without the formation of large aggregates. Rhamnolipid therefore allowed the specific surface area of the nZVI to be kept high and therefore allowed maximum exposure to the Cr(VI). Results also indicate that rhamnolipid had no effect on Cr(VI) concentration and therefore it was entirely the ZVI in its various forms that were responsible for the reduction of Cr(VI) to Cr(III).

Other studies have taken place where nZVI are stabilized using a support material comprising of multi-walled carbon nanotubes (MWNT). The purpose of the MWNT was to act as a cathode whilst the nZVI acted as an anode thereby avoiding the creation of an oxidized film on nZVI (Lv et al, 2011). This proved to be efficient as 100% of chromium appeared to be removed within 2 h

of nZVI-MWNT exposure. Compared to this project, the efficiency of the removal of chromium is more effective using the nZVI-MWNT approach though the ramifications of using MWNT in environmental remediation have the potential to have other human and environmental implications. Carbon nanotubes (CNT) have been used in a variety of technologies such as drug delivery and electronics though the consequences of CNT on the environment are still largely unknown. CNT are shown to a have high aspect ratio such as asbestos and can cause severe lung damage. Due to nZVI being in direct contact with environmental waters, a more eco-compatible surfactant was chosen that is produced naturally by biological organisms which contrasts MWNT, so that no additional contaminants are added into the environment in an attempt to reduce Cr(VI).

4.7 Rate Order Reaction Kinetics of nZVI

With the results obtained from the flame atomic adsorption, it is able to calculate the rate order of the reaction for Cr(VI) reduction by nZVI. Pseudo first order kinetics is described in equation 3.1:

$$\frac{dC}{dt} = -k_{obs}C \qquad \text{Equation 4.2}$$

Where C is the concentration of Cr(VI) in mg that remains left in the aqueous phase and therefore has not been converted to Cr(III). K_{obs} is the rate order constant. Integration of the above equation leads to the following equation:

$$ln\frac{C}{C_0} = -k_{obs}t$$ Equation 4.3

Where Co is the original concentration of Cr(VI) and t is the time at any point. The results from atomic adsorption allow a graph to be plotted of $\ln(C/C_0)$ with respect to time which demonstrates a linear relationship with the slope possessing an R^2 value of 0.97. The atomic adsorption results allow a confirmation that the rate of Cr(VI) reduction by nZVI follows pseudo first order reaction kinetics.

The results from flame atomic adsorption can finalise the rate order kinetics of the reduction of Cr(VI) by micro scale ZVI. The rate does not follow pseudo first order reaction kinetics though does follow second order reaction kinetics, governed by the following equation:

$$\frac{1}{C} - \frac{1}{C_0} = k_{obs}t$$ Equation 4.4

The results from atomic adsorption can be used to plot a graph of $(1/C - 1/C_0)$ with respect to time. This correlation is linear with an R^2 value of 0.96 determining that the reduction of Cr(VI) with micro scale ZVI is a second order reaction.

4.8 Surfactant Selection

There are many surfactants available for use though rhamnolipid was chosen over others for various reasons. AFM results indicate that rhamnolipid was able to disperse nanoparticles so that the mean size of the particles ranged between 20-60 nm. Other surfactants that have been used to disperse nZVI such as Span-85 have created particle sizes ranging from 35-140 nm (Su et al, 2012) which is substantially larger than the nanoparticles created in this project. The increased

size of the particles leads to a decreased specific surface area to be able to react with Cr(VI). Coating of nZVI particles with polymers allows for increased repulsion between nanoparticles overcoming the van der Waal forces between nanoparticles and therefore leading to better stability and dispersion. Two commonly used polymers are carboxymethyl cellulose (CMC) and polyacrylic acid (PAA) which disperses nZVI to have an average diameter of 85 nm and 189 nm respectively using TEM which is substantially higher than the results shown by this project (Cirtiu et al, 2011). Usually polymers decrease the particle size, though these two common polymer surfactants chelate ferrous ions before reduction during synthesis which condenses iron into polymer zones. This can lead to uneven surface coverage which increases particle size and polydispersity. AFM results from this project show a much lower size distribution of nZVI particles giving reason to suggest that rhamnolipid incorporation during the synthesis of nZVI allows for the even distribution of the particles.

Polyacrylamide is also a diversely used polymer and is used as a coating agent to disperse nZVI. Considering that the surfactant stabilized nZVI will be used to remediate Cr(VI) in environmental waters, it is important to ensure that the surfactant does not pose any human or environmental damage. Though polyacrylamide itself is non-toxic, it can potentially release acrylamide which is a toxin that causes damage to nerves and is a human carcinogen. Polyacrylamide can disperse nZVI samples if present during synthesis to achieve a particle size diameter of 55 nm by AFM (Cirtiu et al, 2011) which is similar to this study's AFM particle size results but has the ability to pose a threat to human and environmental health which is why an eco-compatible and biodegradable biological surfactant was chosen as the surfactant of choice in this study to dispersed nZVI nanoparticles.

Polyvinylpyrollidone (PVP) is a water soluble and low cost capping agent used to disperse nZVI as studied by Chen et al, 2011 and can be compared to rhamnolipid surfactant. Particle sizes appeared to be ranging between 10-40 nm with PVP capping agent and between 20-60 nm with rhamnolipid which is not considerably higher. Though PVP is able to lower the size of the nZVI particles which would increase the specific surface area of the particle and provide a larger area to react with Cr(VI), considerations of the surfactants eco-compatibility must be taken into account. A usually inert PVP has the ability to combine to iodine to create an iodophore which possesses disinfectant and antimicrobial activity (Heiner et al, 2010) which can implement a negative influence on microbial organisms residing in environmental waters. This may alter the food chain by decreasing the number of bacteria in environmental waters which act as a food source for a number of larger organisms and consequently disrupting food webs. There is a high probability that PVP would be able to react with iodine as PVP is used as a capping agent for nZVI which would then be exposed to chromium which is used to synthesise various pigments. Iodine may be a part of the same industrial wastewater as chromium as iodine is also incorporated into creating pigments and therefore increasing the chances that iodine could react with PVP-nZVI.

5. Conclusion

By using a ferric reduction synthesis method, nZVI were created either without or with the incorporation of rhamnolipid surfactant. The nanoparticles were then characterized using multiple methods in order to determine the hydrodynamic diameter, size, crystal structure, chemical content as well as the rates of aggregation of the particles with and without the presence of rhamnolipid surfactant. It was hypothesized that nanoparticles without the incorporation of a surfactant would rapidly aggregate to form large sized clusters whilst nanoparticles with the rhamnolipid surfactant would remain dispersed and retain a nano size. It was also hypothesized that nZVI would oxidize with time and gain an iron oxide shell.

The hypotheses were tested by determining the nZVI hydrodynamic diameter, size, crystal structure and chemical content at various time points in order to determine the rate of aggregation and change in chemical composition. It was resolved that nZVI nanoparticles without a surfactant rapidly aggregate from approximately 230 nm to 3 μm in three hours after synthesis and nZVI particles that are incorporated with rhamnolipid are able to maintain dispersion at approximately 50 nm for the same duration of time. It was also found that a fresh sample of nZVI consisted mostly of zero valent iron whilst an aged sample consisted mostly of iron oxide.

Iron has previously been used to convert hazardous Cr(VI) to less toxic Cr(III) by redox reaction. Cr(III) forms a complex with iron and precipitates out of solution thereby lowering the concentration of solution phase Cr(VI). It was hypothesized that rhamnolipid incorporated nZVI would be more efficient at conversion of Cr(VI) to Cr(III) compared to aggregated micro scale nZVI to do the availability of an increased specific surface area provided by rhamnolipid

dispersed nZVI. In order to test the hypothesis, Cr(VI) was reacted with either rhamnolipid dispersed nZVI or aggregated micro scale nZVI for various lengths of time . The concentration of remaining solution phase chromium was measured with flame atomic adsorption spectroscopy in order to measure the rate of removal of solution phase Cr(VI). It was determined that rhamnolipid dispersed nZVI were able to convert solution phase Cr(VI) to Cr(III) at a twelve fold better efficiency compared to aggregated micro scale nZVI in the span of four hours.

6.0 Future Work

Through the findings of this project, a number of ideas for future work can be mentioned. Since the scope of this project focuses the ability of nZVI to potentially remediate hazardous Cr(VI) from environmental waters, it is crucial to further investigate factors that effect the efficiency of nZVI as well as any likely negative impact nZVI may pose to the environment.

1. The use of nZVI has shown to allow the conversion of Cr(VI) to a less dangerous Cr(III) which allows for a decrease in solution phase chromium. Although nZVI has determined to be drastically more effective than aggregated micron size nZVI, further work can be conducted by introducing a bi-metallic nZVI with the incorporation of a second and less reactive metal such as platinum. Platinum is known to trigger the oxidation of iron and could be used as a mechanism to increase the transfer of electrons in the reduction of Cr(VI). To explore this further, nZVI nanoparticles can be soaked in a salt solution of platinum to produce a bi-metallic nZVI which can then be reacted with Cr(VI). Atomic adsorption can then be used to quantify the concentration of chromium that was not converted from the hexa to the tri form in order to determine if the bi-metallic nZVI had a faster rate of reaction compared to only nZVI.
2. It has been established that nZVI has poor mobility and aggregates extremely quickly without the use of a surfactant. Being able to track the transport and fate of nZVI is important so that nZVI can be recovered from the environment after use. The zetasizer has an option to track mobility measurements which can be used to track the transport of nZVI to gain an understanding of how far nZVI can travel in environmental waters under different circumstances. An electrical field will be applied to the particle which will instigate the particles to move at a speed relative to their surface charge. This speed can

be measured and electrophoretic mobility can be determined. This information can provide some insight on how different solutes or ions in solution are able to impact the movement of nZVI which can be used to determine the fate of nZVI in environmental systems where steric stabilisation is not important.

3. It is important to understand the eco-toxicity of nZVI on environmental organisms and at which dose nZVI could be dangerous. Tetrahymena thermophila (T.t) is a protozoa that is abundantly found in fresh water and is often used as a model organisms in eco-toxicity studies. Different concentrations of nZVI can be exposed to T.t in order to determine if nZVI impedes on the regular growth rate of T.t. This information can be used to obtain knowledge on acceptable and environmentally safe concentrations of nZVI that can be used to remediate contaminants. It has been determined that other nanoparticles have been able to alter the regular digestion process of T.t on bacterial E. coli (Nasser et al, 2012) so that the bacteria are encapsulated in vesicles rather than digested. This could lead to an increase in the bacterial population and it is important to consider if nZVI could have similar effects on the digestion of bacteria due to nanoparticle size rather than chemical composition. E-coli bacteria can be linked to a green fluorescent protein (gfp) which only fluoresces if the bacteria are viable. A fluorocytometer can be used to quantitatively measure the amount of fluorescence given off by the bacteria in order to determine if the bacteria are being digested normally in the presence of nZVI or if nZVI is changing the regular feeding pattern of T.t. Confocal microscopy can also be used to image any morphological changes in the T.t caused by nZVI.
4. Considering that nZVI can potentially interact and be ingested by smaller water based organisms, which are preyed on by larger organisms, it is important to be able to track the

fate of nZVI through the food web. T.t is a filter feeder and preys on smaller organisms through an oral apparatus and ingests its surroundings without any bias as to what it ingests. Nanoparticles can be ingested and be preyed upon by larger organisms such as Amoeba. To track the amount of nZVI being passed along the food chain, a known concentration of nZVI can be exposed to T.t which can then ingest the nZVI. Typical time spans for ingestion are approximately 1-3 hours after which the T.t can then be exposed to Amoeba. The Amoeba can then be imaged with confocal microscopy in an attempt to find dark pellets of nZVI. This could quantitatively be determined by linking nZVI to a fluorescent probe which could then be quantitatively tracked through fluorocytometry. This would increase the awareness of how nZVI is able to move through the food chain or if it is excreted out of the primary organism and back into the environment before the primary organism is ingested by a predator. This could also lead to findings on if the nZVI is altered in any way during the consumption process and in what form is it released if the nZVI is excreted back into the environment.

5. This project focussed on synthesis of nZVI, characterization of the ability of nZVI to reduce Cr(VI) to a less toxic Cr(VI) and decreasing solution phase chromium. Another important point to consider are other competing contaminants and the ability of nZVI to degrade them. Industrial effluent can contain a broad range of various contaminants especially hydrocarbons with halogen functional groups, so it is imperative to determine the efficiency of nZVI being able to reduce other chemicals in order to maximize the amount of contaminants that can be degraded by nZVI to make nZVI cost effective. Various hydrocarbon contaminants such as trichloroethylene (TCE) can be exposed to nZVI which would donate electrons and lead to dechlorination of the hydrocarbon. The

efficiency of degradation can be assessed by using gas chromatography where the intensity of the peaks in the chromatography plots would decrease over time if the compound was being degraded. This would allow increase awareness on the full scope of how nZVI can impact a range of contaminants and would also indicate which chemicals are most affected by nZVI.

References

Alidokht A., et al (2011) "Reductive Removal of Cr(VI) by Starch Stabilized Fe^0 nanoparticles in aqueous solution" **Desalination**. Vol. 270: pg 105-110.

Auffan M., et al (2009) "Towards a Definition of Inorganic Nanoparticles from an Environmental, Health and Safety Perspective" **Nature Nanotechnology**. Vol. 4: pg 634-641.

Baalousha M and Lead JR., (2012) "Rationalizing nanomaterial sizes Measured by Atomic Force Microscopy, Field-Flow Fractionation, and Dynamic Light Scattering: Sample Preparation, Polydispersity, and Particle Structure" **Environmental Science and Technology**. Vol 46: pg 6134-6142.

Baalousha M and Lead JR., (2007) "Size Fractionation and Characterization of Natural Colloids and Nanoparticles" **Science of the Total Environment**. Vol. 386: pg 93-102

Barnes RJ., et al (2010) "The Impact of zero-valent iron nanoparticles on a river water bacterial community" **Journal of Hazardous Materials**. Vol. 184: pg 73-80.

Bhushan B., (2004) "Springer Handbook of Nanotechnology" Springer: pg 385-393.

Binning G., et al (1986) "Atomic Force Microscope" **Phys Res Lett**. Vol. 56: pg 930-933.

Boisseau P., Loubaton B., (2011) "Nanomedicine, Nanotechnology in Medicine" **Competes Rendus Physique**. Vol. 12: pg 620-636.

Borkovec M.., (2002) "Analysis and Characterization in Surface Chemistry" John Wiley and Sons. Chapter 18: pg 357-370.

Burbridge DJ., (2012) "Chromium speciation in River Sediment Pore Water Contaminated by Tannery Effluent" **Chemosphere**. Vol. 89: pg 838-843.

Byrappa K., et al (2008) "Nanoparticle Synthesis using Supercritical Fluid Technology-
Towards Biomedical Applications" **Advanced Drug Delivery Reviews**
Vol. 60: pg 299-237.

Cao J., et al (2005) "Perchlorate Reduction by Nanoscale Iron Particle" **J. Nanoparticle Res**. Vol. 7: pg:499-506.

Chen H., et al (2011) "Removal of Tetracycline from aqueous solutions using polyvinylpyrrolidone (PVP-K30) modified nanoscale zero valent iron" **Journal of Hazardous Materials**. Vol. 192: pg 44-53.

Chen KF., et al (2011) “Renewable Hydrogen Generation by Bimetallic Zero Valent Iron Nanoparticles” **Chemical Engineering Journal**. Vol. 170: pg 562-567.

Chen TH., et al (2011) “Behavioural Effects of Titanium Dioxide Nanoparticles on Larval Zebrafish” **Marine Pollution Bulletin**. Vol. 63: pg 303-308.

Ciacci C., et al (2012) “Effects of Sublethal, environmentally relevant concentrations of hexavalent chromium in the gills of Mytilus galloprovincialis” **Aquatic Toxicology**. Vol. 120: pg 109-118.

Cirtiu CM., et al (2011) “Systematic Comparison of the size, surface characteristics and colloid stability of zero valent iron nanoparticles pre- and post-grafted with common polymers” **Colloids and Surfaces A: Physiochem. Eng. Aspects.** Vol. 390: pg 95-104.

Compano R and Hullmann A., (2002) “Forecasting the Development of Nanotechnology with the help of Science and Technology Indicators” **Nanotechnology**. Vol. 13: pg 243-247.

Crane RA., et al (2011) “Magnetite and zero valent iron nanoparticles for the remediation of uranium contaminated environmental water” **Water Research**. Vol. 45: pg 2931-2942.

Crane RA and Scott TB., (2012) “Nanoscale Zero Valent Iron: Future Prospects for an Emerging Water Treatment Technology” **Journal of Hazardous Materials**. Vol. 211: pg 112-125.

Dill KA and Bromberg S., (2002) “Molecular Driving Forces: Statistical Thermodynamics in Chemistry and Biology” **Garland Science**. New York, New York.

Dong YD and Boyd BJ., (2011) “Applications for X-Ray Scattering in Pharmaceutical Science” **International Journal of Pharmaceuticals**. Vol. 417: pg 101-111.

Dong H and Lo IM., (2012) “Influence of Humic Acid on the Colloid Stability of Surface-modified nano zero valent iron” **Water Research**. pg: 1-9.

Drmosh QA., et al (2010) “Spectroscopic Characterization approach to study surfactant on ZnO_2 nanoparticles synthesis by laser ablation process” **Applied Surface Science**. Vol. 256: pg 4661-4666.

Du H and Yu F., (2006) “Role of the Binary H_2SO_4 homogenous nucleation in the formation of Volatile Nanoparticles in the Vehicular Exhaust” **Atmospheric Environment**. Vol. 40: pg 7579-7588.

European Commission: Health and Consumer Protection Directorate-General. C7 Risk Assessment (2003).

European Commission (2011) Recommendations of defining a Nanomaterial.

Ferreira SL., et al (2001) “On-line Preconcentration system for Nickel Determination in Food Samples using Flame Atomic Absorption Spectroscopy” **Anaytical Chemica Acta**. Vol. 445: pg 145-151.

Goulle JP., et al (2012) “Accidental Potassium Dichromate Poisoning. Toxicokinetics of Chromium by ICP-MS-CRC in Biological Fluids and in Hair” **Forensic Science International**. Vol. 217: pg e8-e12.

Guzman KAD., et al (2006) “Environmental Risks of Nanotechnology: National Nanotechnology Initiative Funding 2000-2004” **Environ. Sci. Technol**. Vol 40: pg 1401-1407.

Gondal MA., et al (2012) “Synthesis of Nickel-Oxide nanoparticles using Pulsed Laser Ablation in Liquids and their Optical Characterization” **Applied Surface Science**. Vol. 258: pg 6982-6986.

Healy TW and Fuerstenau DW., (2007) “The Iso-electric point/Point of zero charge Interfaces formed by aqueous solutions and nonpolar solids, liquids and gases” **Journal of Colloid and Interface Science**. Vol. 309: pg 183-188.

Heiner JD., et al (2010) “10% Povidone-Iodine may be a Practical Field Water Disinfectant” **Wilderness and Environmental Medicine**. Vol. 21: pg 332-336.

Ihee H., et al (2005) “Ultrafast X-Ray Diffraction of Transient Molecular Structures in Solution” **Science**. Vol. 309: pg 1223-1226.

Ikai A., (2008) “Nanobiomechanics of Proteins and Biomembrane” **Philos. Trans. R. Soc. Lond. B Biol. Sci.** Vol. 363: pg 2163-2171.

Ikai A., (2008) “The world of Nano-Biomechanics: Mechanical Imaging by Atomic Force Microscopy” Elsevier. Amsterdam.

Izbicki JA., et al (2008) “Chromium, chromium Isotopes and Selected Trace Elements, Western Mojave Dessert” **Applied Geochemistry**. Vol. 23: pg 1325-1352.

Jabs T., (1999) “Reactive Oxygen Intermediates as Mediators for Programmed Cell Death in Plants and Animals” **Biochem Pharmacol**. Vol. 57: pg 231-235.

Kanimozhi G., et al (2011) “Umbelliferone Modulates Gamma Radiation Induced Reactive Oxygen Species and Subsequent Oxidative Damage in Human Blood Lymphocytes” **European Journal of Pharmacology**. Vol. 672: pg 20-29.

Karchemski F., et al (2012) “Carbon-nanotube liposomes conjugate as a Platform for Drug Delivery into Cells” **Journal of Controlled Release** Vol. 160: pg 339-345.

Kaushik N., (2010) “Biological Synthesis of Metallic Nanoparticles” **Nanomedicine: Nanotechnology, Biology and Medicine**. Vol. 6: pg 257-262.

Kelkar AV., et al (2013) “New models and Predictions for Brownian Coagulation of non-interacting spheres” **Journal of Colloid and Interphase Science**. Vol. 389: pg 188-198.

Kreyling WG., et al (2010) “A complementary Definition of Nanomaterial” **Nano Today**. Vol. 5: pg 165-168.

Lee C and Sedlack DL., (2008) “Enhanced Formation of Oxidants from Bimetallic Nickel-Iron Nanoparticles in the Presence of Oxygen” **Environ. Sci. Technol.** Vol. 42: pg 8528-8533.

Li XQ., et al (2006) “Zero valent iron nanoparticles for the abatement of Environmental Pollutants: Materials and Engineering Aspects” **Critical Reviews in Solid State and Materials Science**. Vol. 3: pg 111-122.

Lienado RA and Neubecker TA., (1983) “Surfactants” **American Chemical Society**. Vol. 55: pg 93-101.

Linos A., et al (2011) “Oral Ingestion of hexavalent chromium though drinking water and cancer mortality in an Industrial area of Greece- An Ecological Study” **Environmental Health**. Vol 10: 50.

Liu L and Wei., (2012) “Influence of Photoirradiation on reduction of Hexavalent Chromium by zero-valent iron in the presence of organic acids” **Desalination**. Vol. 285: pg 271-276.

Liu Y., et al (2011) “Intracellular Dynamics of cationic and anionic polystyrene nanoparticless without direct interaction with mitotic spindle fibres” **Biomaterials**. Vol. 32: pg 8291-8303.

Lv X., et al (2011) “Removal of chromium(VI) from wastewater by Nanoscale Zero valent Iron Nanoparticles Supported on Multi Walled Carbon Nanotubes” **Chemosphere**. Vol. 85: pg 1204-1209.

Malvern Instruments Limited (2012). http://www.malvern.com/labeng/technology/dynamic_light_scattering/dynamic_light_scattering.htm

Metcalf IM and Healy TW., (2012) “The electrokinetic properties of Colloidal Magnetic Iron Oxides” **American Chemical Society**. Vol. 28: pg 7897-7903.

Nasser F., et al (2012) “Carbon Nanotubes compared with Carbon Black: Effects on Bacterial Survival Against Grazing by Cilliates and Antimicrobial Treatments” **Nanotoxicology**. Early Online : pg 1-8.

Patra RC., et al (2010) "Molecular Characterization of Chromium (VI) Reducing Potential in Gram Positive Bacteria Isolated from Contaminated Sites" **Soil Biology & Biochemistry** Vol. 42: pg 1857-1863.

Permenter MG., et al (2011) "Exposure to Nickel, Chromium or Cadmium Causes Distinct Changes in the Gene Expression Patterns of a Rat Liver Derived Cell Line" **PLOS ONE**. Vol. 6: pg 1-11.

Pishkenari HN., et al (2006) "Acquisition of high-precision Images for non-contact Atomic Force Microscopy" **Mechatronics** Vol. 16: pg 655-664.

Ponder SM., et al (200) "Remediation of Cr(VI) and Pb(II) Aqueous Solutions using Supported Nanoscale Zero-valen Iron" **Environ. Sci. Technol.** Vol. 34: pg 2564-2569.

Prete AD., et al (2008) "Role of Mitochondria and Reactive Oxygen Species in Dendritic Cell Differentiation and Functions" **Free Radical Biology and Medicine**. Vol. 44: pg 1443-1451.

Quang DV., et al (2011) "Preparation of Amino Functionalized silica micro beads by dry Method for Supporting Silver Nanoparticles with Antibacterial Properties" **Colloids and Surfaces A: Physiochemical and Engineering Aspects"** Vol. 389: pg 118-126.

Raychoudhury T., et al (2012) "Aggregation and Deposition Kinetics of Carboxymethyl Cellulose modified zero-valent iron nanoparticles in porous media" **Water Research**. Vol. 46: pg 1735-1744.

Reimer L and Khol H., (1997) "Transmission Electron Microscopy" Springer Series in Optical Sciences. 5th edition.

Rochow TG and Tucker PA., (1994) "Introduction to Microscopy by Means of Light, Electrons, X Rays or Acoustics" 2nd edition. Plenum Press.

Rusch B., et al (2010) "Coating of Quarz silica with iron oxides: Characterization and Surface Reactivity of iron coating phases" Vol. 353: pg 172-180.

Salaun MC and Salaun P., (2007) "Quantitative determination of hexavalent chromium aqueous solutions by UV-vis spectrophotometer" **Central European Journal of Chemistry**. Vol. 5: pg 1084-1093.

Scintag Inct (1999) http://epswww.unm.edu/xrd/xrdbasics.pdf

Shi X., et al (1999) "Reduction of Chromium (VI) and its Relationship to Carcinogenesis" **J Toxicol Environ Health B Crit Rev**. Vol. 2: pg 87-104.

Singh R., et al (2011) “Synthesis, characterization and the role of zero-valent iron nanoparticle in removal of hexavalent chromium from chromium spiked soil” **J Nanopart Res**. Vol. 13: pg 4063-4073.

Soberon-Chavez G., et al (2005) “Production of Rhamnolipids by Pseudomonas Aeruginosa” **Appl. Microbiol. Biotechnol**. Vol 68: pg 718-725.

Su C., et al (2012) “A two and a half year performance evaluation of a field test treatment of source zone tetrachloroethene and its chlorinated daughter products using emulsified zero valent iron nanoparticles” **Water Research**. Vol. 46: pg 5071-5084.

Subramanian V., Lee T., (2012) “Nanotechnology-Based Flexible Electronics” **Nanotechnology** Vol. 23

Thakkar KN., et al (2010) “Biological Synthesis of Metallic Nanoparticles” **Nanomedicine: Nanotechnology, Biology and Medicine**. Vol. 6: pg 257-262.

Thieme J and Niemeyer J., (1998) “Interaction of Colloidal Soil Particles, Humic Substances and Cationic Detergents studied by X Ray Microscopy” **Struc. Dynam and Prop. Colloid Sys**. Vol. 111: pg 193-201.

Tombacz E and Rice JA., (1999) “Changes of Colloidal State in Aqueous Systems of Humic Acids” Understanding Humic Substances: Advanced Methods, Properties and Applications. Royal Chemistry Society. Cambridge. Pg. 69-77.

Tominaka S., et al (2010) “Nanostructured Catalyst with Hierarchical Porosity and Large Surface Area for on chip fuel cells” **Journal of Power Sources**. Vol. 195: pg 1054-1058.

Twyman RM., (2005) **Microscopy Applications/ Food**: pg 50-57.

Upstone SL (2000) “Ultraviolet/ Visible Light Absorption Spectrophotometry in Clinical Chemistry” Encyclopedia of Analytical Chemistry. John Wiley and Sons: pg 1699-1714.

Vogel TM., Criddle CS., McCarty PL., (1987) “Transformations of Halogenated Aliphatic Compounds” **Environmental Science and Technology** . Vol. 21: pg 722-236.

Whittleston RA., (2009) “Chromium Contamination: A Process Affecting Subsurface Contaminant Mobility” **Earth and Environment**. Vol. 4: pg 83-113.

Xiaoshu Lv., et al (2011) “Removal of Chromium(VI) from wastewater by nanoscale zero-valent iron particles supported on multi-walled carbon nanotubes” **Chemosphere**. Vol. 85: pg 1204-1209.

Xie Y., et al (2006) “Synthesis of silver nanoparticles in Reverse Micelles stabilized by Natural Biosurfactant” **Colloids and Surfaces: Physiochem Engineering Aspects**

Ye S., et al (1999) “Role of Reactive Oxygen Species and p53 in Chromium (VI)-induced Apoptosis” **The Journal of Biological Chemistry**. Vol. 274: pg 3474-3480.

Yin K., et al (2012) “Lab Scale Stimulation of the fate and transport of nano-zero valent iron in subsurface environments: Aggregation, sedimentation and contaminant desorption” **Journal of Hazardous Materials**. Vol. 227: pg 118-125.

Yuvakkumar R., et al (2011) “Preparation and Characterization of Zero Valent Iron Nanoparticles” **Digest Journal of Nanomaterials and Biostructures**. Vol. 6: pg 1771-1776,

Zhang WX and Elliot DW., (2006) “Applications of Iron Nanoparticles for Groundwater Remediation” **Remediation**. Vol. 16: pg 7-21.

Zhang M., et al (2011) “Degradation of soil-sorbed tricholoroethylene by stabilized zero valent iron nanoparticles: effects of sorption, surfactants and natural organic matter” **Water Research**. Vol. 45: pg 2401-1414.

Zhang W., (2003) “Nanoscale Iron Particles for Environmental Remediation” **J. Nanopart. Res** Vol. 5: pg 323-332.

Zou X., et al (2011) “Electron Crystallography: Electron Microscopy and Electron Diffraction” Oxford Science Publications.